Technical Report 347

Probability Distribution of Antenna Gain for Satellite with Switched Antenna System

R. N. Assaly

4 February 1964

Lincoln Laboratory

MASSACHUSETTS INSTITUTE OF TECHNOLOGY

Lexington, Massachusetts

MASSACHUSETTS INSTITUTE OF TECHNOLOGY

LINCOLN LABORATORY

PROBABILITY DISTRIBUTION OF ANTENNA GAIN FOR SATELLITE WITH SWITCHED ANTENNA SYSTEM

R. N. ASSALY

Group 61

TECHNICAL REPORT 347

4 FEBRUARY 1964

LEXINGTON   MASSACHUSETTS

ABSTRACT

For a communication system using satellites carrying antennas tied to a switching system, the probability distribution of angles between the pointing directions of the axis of the operating antenna and of a ground receiving station is found. This study is based on the condition that the antenna pointing most nearly in the direction of a sensing signal is switched on. In the determination of the characteristics of this system, geometries of pointing directions are found, which are optimum or near optimum, for the cases of 4, 6, 8, 12, 16, 24, 32, 48, and 60 antennas. Consideration is also given to determining an optimum antenna pattern to be used with any geometry. For any pattern, a conversion from probability distribution of angles to probability distribution of gains is straightforward. The results of this study are summarized in a chart.

TABLE OF CONTENTS

PROBABILITY DISTRIBUTION OF ANTENNA GAIN FOR SATELLITE WITH SWITCHED ANTENNA SYSTEM

I. INTRODUCTION

A communication system is presently being studied that employs a number of active satellites dispersed in separate near-synchronous orbits about the earth. Each satellite will have an array of antennas only one of which will radiate at any one time during operation. The satellite must carry instrumentation to monitor a signal from the earth and switch on the antenna that points most nearly in the direction of the signal. On the other hand, the need of satellite stabilization is eliminated. Without describing equipment design, this report discusses arrangements of various numbers of antenna pointing directions and the antenna gains in the direction of an earth receiving station. The RF power that must be generated in the satellite should be as low as possible, whereas the power transmitted from a ground station can be sufficiently high so that the location of the transmitter may be eliminated as a factor.

The direction-sensing system that provides the logic for determining which antenna to switch on may be designed to monitor the signal from the transmitter, a signal sent from the receiving station or, if an infrared system is used, the signal arriving apparently from the center of the earth. This direction will be denoted as OS with the satellite situated at O, as shown in Fig. 1.

The satellite carries N antennas all of which will be assumed to have the same circular symmetric antenna pattern. The pointing directions of the centers of their patterns will be denoted by OT_n (n = 1, 2, ..., N) and that of the antenna in operation by OT.
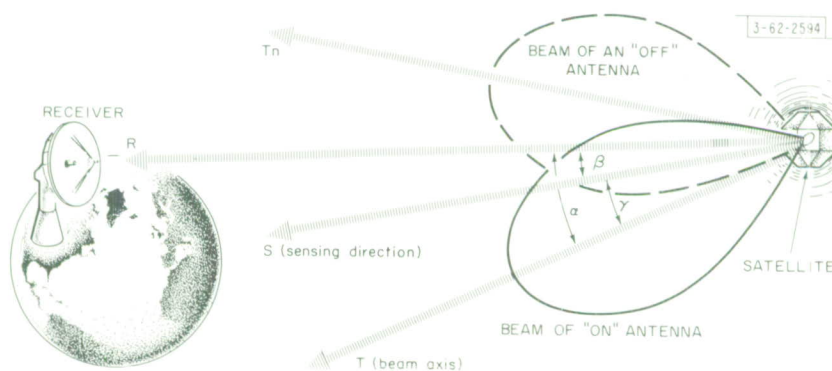

Fig. 1. Schematic view of communication system showing operation of one satellite O. The signal sensed propagates along direction OS and the antenna whose pointing direction OT is most nearly in direction OS is switched on. The receiver is in the direction OR.

1

Other designations will be

> OR (direction of the receiving station),
>
> α (angle between OR and OT),
>
> β (angle between OR and OS),
>
> γ (angle between OT and OS).

In normal operation, it can be assumed that of the directions OT_n, OT subtends the smallest angle with OS, that is, the antenna pointing most nearly in the direction of the signal sensed will be the one in operation. Hence, the region enclosing the satellite can be pictured as divided into pyramidal segments by planes, each of which bisects the angle between two adjacent directions OT_n and is normal to the plane in which the two OT_n lie. Each segment defines the region in which OS must lie for the corresponding antenna to operate.

It is apparent that for any geometry of the pointing directions OT_n, angle γ has a maximum value v_m. Furthermore, the maximum value of angle α would be $\beta + v_m$. In mathematical terms

$$P(\alpha < a) = 1 \quad , \quad a > \beta + v_m \tag{1a}$$

or

$$P(\alpha < a) < 1 \quad , \quad a < \beta + v_m \quad . \tag{1b}$$

One would want to choose the geometry that gives the lowest values of v_m. This allows the antennas to be designed for narrower beamwidths and correspondingly higher gains. The RF power source requirements would then be lessened.

The concept of the system and its operation has now been made clear. To resolve the value of the system, the discussion will follow the procedure outlined below:

(a) Development of the general equations to determine the probability distribution $P(\alpha < a)$, the probability that angle α is less than various angles a for various values of angle β.

(b) Programming the equations for calculation by a computer.

(c) Selection of pointing direction geometries for different numbers of antennas that will give minimum or near-minimum values of v_m. The cases that are explored are N = 4, 6, 8, 12, 16, 24, 32, 48, and 60 antennas.

(d) Calculation and plot of $P(\alpha < a)$ for these geometries.

(e) Determination of the optimum antenna for these geometries based on a representative antenna pattern $g = 2J_1(g_0 \sin \alpha)/\sin \alpha$.

(f) Consideration of the RF circuits supplying the antennas and estimation of the circuit losses.

The results of this discussion are summarized in Figs. 6 to 24, Fig. 27, and Appendix A.

II. DEVELOPMENT OF THE EQUATIONS FOR $P(\alpha < a)$

Consider an arbitrary pyramidal segment (Fig. 2). Introduce an incremental sheet bound by two cones, $TOS° = \gamma$ and $TOS° = \gamma + d\gamma$, and the boundary planes of the segment. The probability that OS will fall within the strip is

$$P_s = \frac{\Omega}{4\pi} \quad , \tag{2}$$

2

Fig. 2. Geometry associated with antenna in operation. It is characterized by a segment of a sphere whose boundary is made up of planes bisecting the angles between adjacent pointing directions.
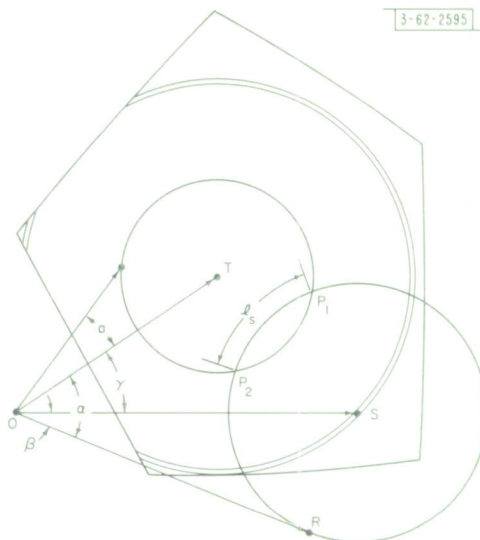
where Ω is the solid angle enclosed and 4π is the solid angle of the whole celestial sphere. (This is based on the condition that all directions OS are equally probable.) In turn, the solid angle Ω is the product of the angular length ℓ_t and angular width $d\gamma$. Hence,

$$P_s = \frac{\ell_t \, d\gamma}{4\pi} \quad . \tag{3}$$

Angle ℓ_t is measured on the surface of the cone TOS° $= \gamma$ at its apex (as if the cone surface were slit along a generator line and unrolled before the measurement). This surface is sliced by the boundary of the pyramidal segment, and ℓ_t is the sum of the angles of the surface sectors inside the boundary.

For any direction OS, direction OR will fall on the surface of another cone whose axis is OS, since the angle ROS° $= \beta$ is invariant. (Each value angle β assumes may be viewed as an independent situation.) The probability that $\alpha < a$ is

$$P_a = \frac{\ell_s}{\ell_c} \quad , \tag{4}$$

where ℓ_s is the angle of the sector measured on the surface of the cone ROS° $= \beta$ for which $\alpha < a$ and ℓ_c is the total angle of the cone surface measured at its apex. (This is based on the condition that all directions OR, where ROS° $= \beta$, are equally probable.)

The probability that direction OS lies within the incremental sheet and $\alpha < a$ is

$$P' = P_s P_a = \frac{\ell_t \ell_s \, d\gamma}{4\pi \ell_c} \quad . \tag{5}$$

If direction OS fell within any other incremental sheet, the probability would be given by the same formula, the values of ℓ_t and ℓ_s being different. The probability that $\alpha < a$ for any direction OS must then be the sum of the individual probabilities, or

$$P(\alpha < a) = \sum \frac{\ell_t \ell_s \, d\gamma}{4\pi \ell_c} \quad .$$

The summation over one pyramidal segment is, in the limit, an integration. The sum over all segments is a sum of the integrals. So

$$P(\alpha < a) = \sum_{n=1}^{N} \int \frac{\ell_t \ell_s \, d\gamma}{4\pi \ell_c} \quad , \tag{6}$$

where n denotes the nth segment. The summation can be carried out over all the segments for the same angle γ before integrating. Angle ℓ_t would be the only factor that could change from one segment to another. The formula can then be given finally as

$$P(\alpha < a) = \frac{1}{4\pi} \int \left(\frac{\ell_s}{\ell_c}\right)\left(\sum_{n=1}^{N} \ell_{tn}\right) d\gamma \quad . \tag{7}$$

It remains to find expressions for ℓ_s/ℓ_c and ℓ_{tn} .

For ℓ_s/ℓ_c, Fig. 3(a-f) shows the various possible situations that may exist and the value of ℓ_s/ℓ_c which corresponds to each situation. Four of the cases are self evident; the other two, $a - \beta < \gamma < a + \beta$, $a > \beta$ and $\beta - a < \gamma < a + \beta$, $a \leqslant \beta$ are derived in Appendix B.

3-62-2596

(a) $\gamma \geq a + \beta$
$\dfrac{\ell_s}{\ell_c} = 0$

(b) $\gamma \geq a + \beta$
$\dfrac{\ell_s}{\ell_c} = 0$

(c) $a - \beta < \gamma < a + \beta$
$\dfrac{\ell_s}{\ell_c} = \dfrac{1}{\pi} \cos^{-1} \dfrac{\cos a - \cos \beta \cos \gamma}{\sin \beta \sin \gamma}$

(d) $\beta - a < \gamma < a + \beta$
$\dfrac{\ell_s}{\ell_c} = \dfrac{1}{\pi} \cos^{-1} \dfrac{\cos a - \cos \beta \cos \gamma}{\sin \beta \sin \gamma}$

(e) $\gamma \leq a - \beta$
$\dfrac{\ell_s}{\ell_c} = 1$

(f) $\gamma \leq \beta - a$
$\dfrac{\ell_s}{\ell_c} = 0$
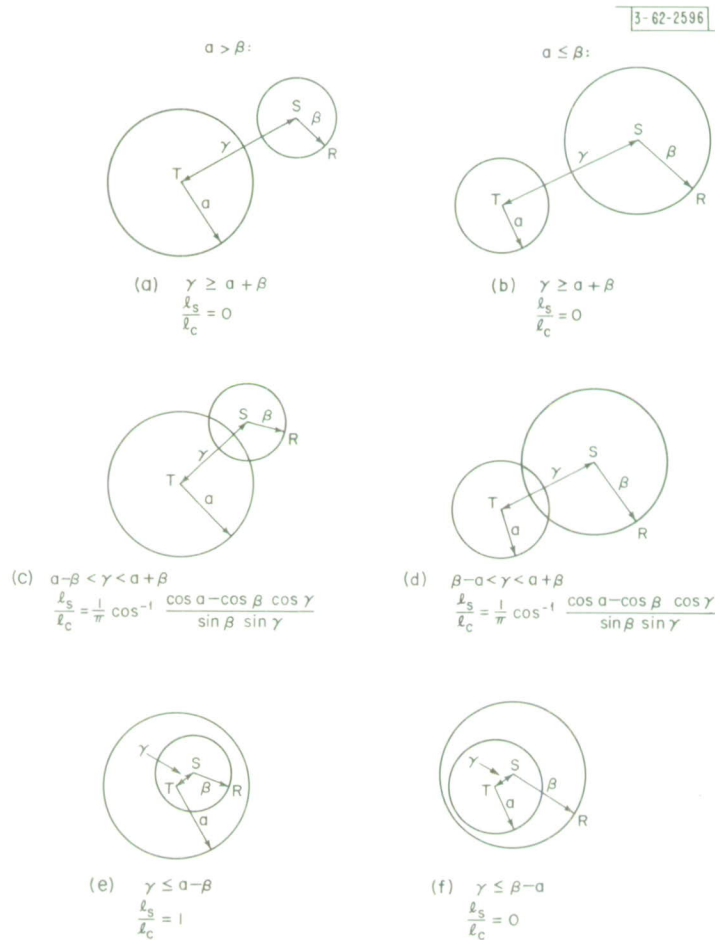
Fig. 3. Various situations that may exist for the relative values of the angles a, β, and γ. The value ℓ_s/ℓ_c is given in each case.
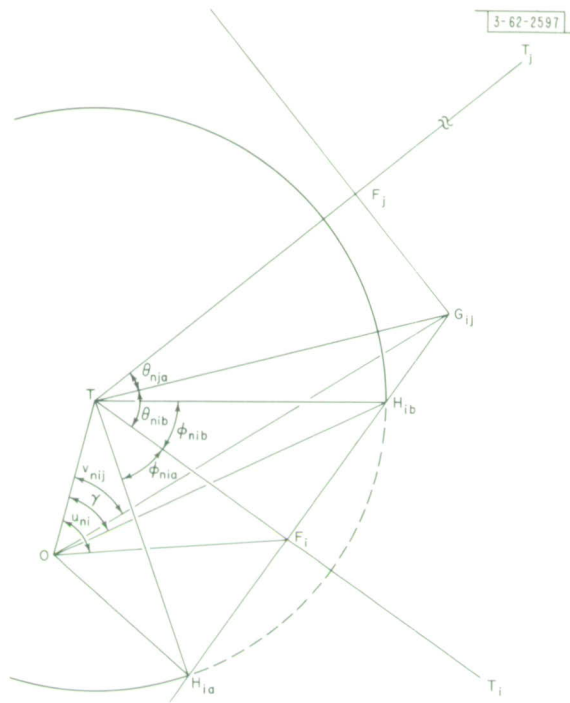
4

Fig. 4. A detailed portion of the geometry of Fig. 2 for the purpose of determining ℓ_{tn}.

To derive the equations for ℓ_{tn}, a geometry for one segment is set up as shown in Fig. 4. The segment belongs to direction OT, and its boundary planes are determined by adjacent directions OT_i ($i = 1, 2, \ldots, I$) with i increasing as one goes counterclockwise around the line OT. Thus, in Fig. 4, $j = i + 1$, or if $i = I$, $j = 1$. The ith boundary plane bisects the angle between the lines OT and OT_i and intersects the plane containing the lines at right angle along the line OF_i. Furthermore, adjacent boundary planes intersect along lines OG_{ij}. The cone defined by $TOS° = \gamma$ may intersect the ith boundary plane along lines OH_{ia} and OH_{ib}. The subscripts a and b will be used to denote the one or the other side of the line OF_i. Let points T, T_i, T_j, F_i, F_j, G_{ij}, H_{ia}, and H_{ib} all lie on a plane which is perpendicular to direction OT. In addition, there are the designations $TOF_i° = u_{ni}$, $TOG_{ij}° = v_{nij}$, $F_iTH_{ia}° = \varphi_{nia}$, $F_iTG_{ij}° = \Theta_{nib}$, as shown in Fig. 4, and $T_iOT_j° = 2u_{nij}$. Also, $TF_iG_{ij}° = \pi/2$.

One starts with the knowledge of the direction cosines of OT (x_n, y_n, and z_n) and OT_i (x_{ni}, y_{ni}, and z_{ni}). Thus,

$$\cos 2u_{ni} = x_n x_{ni} + y_n y_{ni} + z_n z_{ni} \quad , \tag{8a}$$

$$\cos 2u_{nij} = x_{ni} x_{nj} + y_{ni} y_{nj} + z_{ni} z_{nj} \quad , \quad \text{etc.} \tag{8b}$$

The cone $TOS° = \gamma$ intersects the plane TT_iT_j along a circle whose circumference is $2\pi\, TH_{ib}$. The part of the circle within the boundary has length

$$s = 2\pi\, TH_{ib} - \sum_{i=1}^{I} \overline{H_{ia}H_{ib}} \quad , \tag{9}$$

5

where $\overparen{H_{ia}H_{ib}}$ is the length of the arc outside the segment. The angle ℓ_{tn} is then

$$\ell_{tn} = \frac{s}{OH_{ib}} = \frac{2\pi TH_{ib} - \sum\limits_{i=1}^{I} \overparen{H_{ia}H_{ib}}}{OH_{ib}} \quad . \tag{10}$$

But

$$TH_{ib} = OH_{ib} \sin\gamma \tag{11}$$

and

$$\overparen{H_{ia}H_{ib}} = TH_{ib}(\varphi_{nia} + \varphi_{nib}) \tag{12}$$

$$= OH_{ib}(\varphi_{nia} + \varphi_{nib}) \sin\gamma \quad . \tag{13}$$

Hence,

$$\ell_{tn} = \left[2\pi - \sum\limits_{i=1}^{I} (\varphi_{nia} + \varphi_{nib}) \right] \sin\gamma \quad . \tag{14}$$

There are several situations that must be considered.

(a) If $\gamma \leqslant u_{ni}$, then $\varphi_{nia} = \varphi_{nib} = 0$. $\tag{15}$

(b) If $u_{ni} < \gamma < v_{nij}$, then $\varphi_{nib} = \cos^{-1} \dfrac{TF_i}{TH_{ib}}$. $\tag{16}$

But

$$TF_i = OT \tan u_{ni} \tag{17}$$

and

$$TH_{ib} = OT \tan\gamma \quad . \tag{18}$$

Hence,

$$\varphi_{nib} = \cos^{-1} \frac{\tan u_{ni}}{\tan\gamma} \quad . \tag{19}$$

(c) If $\gamma \geqslant v_{nij}$, then $\varphi_{nib} + \varphi_{nja} = \Theta_{nib} + \Theta_{nja}$. $\tag{20}$

Whenever this is the case, the angle φ_{nib} will add with the angle φ_{nja} in Eq. (14) and it is unnecessary to determine them separately. The value of the sum is found by the same procedure that is given in Appendix B. The correspondences in the two cases are

$$OS \rightarrow OT \quad ,$$

$$P_1 ST^\circ \rightarrow T_i TT_j^\circ = \Theta_{nib} + \Theta_{nja} \quad ,$$

$$\beta \rightarrow 2u_{ni} \quad ,$$

$$\gamma \rightarrow 2u_{nj} \quad ,$$

and

$$a \rightarrow 2u_{nij} \quad .$$

Then

$$\varphi_{nib} + \varphi_{nja} = \cos^{-1}\left(\frac{\cos 2u_{nij} - \cos 2u_{ni} \cos 2u_{nj}}{\sin 2u_{ni} \sin 2u_{nj}} \right) \quad . \tag{21}$$

The value of angle v_{nij} is derived in Appendix C and is given by

$$\tan^2 v_{nij} = \frac{2(1 - \cos 2u_{ni})(1 - \cos 2u_{nj})(1 - \cos 2u_{nij})}{1 - \cos^2 2u_{ni} - \cos^2 2u_{nj} - \cos^2 2u_{nij} + 2\cos 2u_{ni}\cos 2u_{nj}\cos 2u_{nij}} . \qquad (22)$$

In summary, the desired probability distribution is given by substituting the value of ℓ_{tn}, Eq. (14), into Eq. (7) and is

$$P(\alpha < a) = \frac{1}{4\pi} \int \left(\frac{\ell_s}{\ell_c}\right) \sum_{n=1}^{N} \left[2\pi - \sum_{i=1}^{I} (\varphi_{nia} + \varphi_{nib})\right] \sin\gamma \, d\gamma$$

$$= \int \left(\frac{\ell_s}{\ell_c}\right) \left[\frac{N}{2} - \frac{1}{4\pi} \sum_{n=1}^{N} \sum_{i=1}^{I} (\varphi_{nia} + \varphi_{nib})\right] \sin\gamma \, d\gamma . \qquad (23)$$

The values of ℓ_s/ℓ_c are given in Fig. 3, and those of φ_{ni} are given by Eqs. (15), (19) or (21). Note that the value of I may change with the value of n. The computation may be simplified if n_1 of the segments are alike, another n_2 are alike, and so on. Then

$$\sum_{m=1}^{M} n_m = N \qquad (24)$$

and

$$P(\alpha < a) = \int \frac{\ell_s}{\ell_c} \left[\frac{N}{2} - \frac{1}{4\pi} \sum_{m=1}^{M} n_m \sum_{i=1}^{I} (\varphi_{mia} + \varphi_{mib})\right] \sin\gamma \, d\gamma . \qquad (25)$$

The values φ_{mi} are the values of φ_{ni} for the n_m-like segments. Similarly, values u_{mi} and v_{mij} will be used for the values of u_{ni} and v_{nij}, respectively.

The limits of integration need only be over the range of angle γ, where the integrand is finite. The lower limit γ_ℓ is then dependent on the factor ℓ_s/ℓ_c and by reference to Fig. 3, its value is

$$\gamma_\ell = 0 \qquad \text{if} \quad a > \beta \qquad (26a)$$

and

$$\gamma_\ell = \beta - a \qquad \text{if} \quad a \leqslant \beta . \qquad (26b)$$

If $\gamma \geqslant a + \beta$, then $\ell_s/\ell_c = 0$, or if $\gamma \geqslant v_m$, where v_m is the largest value of v_{mij} for all values of m or i, then $\sum_i (\varphi_{mia} + \varphi_{mib}) = 2\pi$, and the integrand is 0. The upper limit of γ is then

$$\gamma_u = a + \beta \qquad \text{if} \quad a + \beta \leqslant v_m \qquad (27a)$$

or

$$\gamma_u = v_m \qquad \text{if} \quad a + \beta > v_m . \qquad (27b)$$

Since the largest value angle γ can have is v_m, the range of values of angle α is 0 to $\beta + v_m$. For $a > \beta + v_m$, $P(\alpha < a) = 1$.

III. PROGRAMMING THE EQUATIONS FOR COMPUTER CALCULATION

The difficulties of programming the equations for $P(\alpha < a)$ occur mainly in the formulation of the sum $\sum\limits_{i=1}^{I} (\varphi_{mia} + \varphi_{mib})$. A sensible approach is indicated in the following scheme.

Having a value of γ, we determine whether it is larger than each of the values of v_{m12}, v_{m23}, v_{m34}, etc., in turn. In each case where γ is larger, the corresponding value of $\varphi_{mib} + \varphi_{mja}$ [Eq. (21)] is found and added. Then we compare the value of γ with each of the values of u_{m1}, u_{m2}, u_{m3}, etc. If γ is smaller, there is no contribution [Eq. (15)]. If, for example, the value of γ is larger than u_{m3}, both values φ_{m3a} and φ_{m3b} may contribute to the sum. If $\gamma \geqslant v_{m23}$, the contribution of φ_{m3a} has already been taken up in the first step. Similarly, if $\gamma \geqslant v_{m34}$, the same is true for φ_{m3b}. If $\gamma < v_{m23}$, the contribution of φ_{m3a} is $\cos^{-1}(\tan u_{m3}/\tan \gamma)$ [Eq. (19)]. Also, if $\gamma < v_{m34}$, the contribution of φ_{m3b} is $\cos^{-1}(\tan u_{m3}/\tan \gamma)$. The net contribution then is

$$\varphi_{m3a} + \varphi_{m3b} = \epsilon_{m3} \cos^{-1} \frac{\tan u_{m3}}{\tan \gamma} , \tag{28}$$

where ϵ_{m3} may have the values of 0, 1 or 2. In a program, one can start with the values, $\epsilon_{mi} = 2$, for all m and i. Then, if it is found that $\gamma \geqslant v_{mij}$, the values of ϵ_{mi} and ϵ_{mj} are each decreased by 1. This produces the right contribution for the sum as given, for example, by Eq. (28).

A flow chart for a satisfactory program is given in Appendix D. The data that are read into the program include the pointing directions OT_n needed to define one segment of each different configuration.

IV. SELECTION OF POINTING DIRECTION GEOMETRIES

As indicated in Sec. I, angle γ has a maximum value v_m for any geometry, and the most desirable geometry is the one that gives the smallest value of v_m, permitting the antenna to be designed for minimum beamwidth and consequently maximum gain. However, no method is known for finding the optimum geometry for the general case of N antennas. The procedures outlined in this section for various numbers N may not give the optimum geometry, but in each case, it can be demonstrated that the geometry is sufficiently near optimum that the loss in quality is small.

For this study, the pointing directions will be represented by points T_n ($n = 1, 2, \ldots, N$) on the surface of a sphere of unit radius, where they are actually the vectors joining the sphere center to these points. The sensing direction will be represented by another point S on the sphere surface which is free to wander anywhere among the points T_n. The nearest of the points to point S is the one that defines angle γ. As point S wanders, it will see locations of maximum γ values, such as point G_{ij} in Fig. 4. Each of these locations is spaced by three equal angles from the three neighboring points of the set T_n. For if one travels away from this location in any direction, angle γ decreases. The N points may then be joined by lines on the sphere surface to form a polyhedron whose faces are spherical triangles, and the number of vertices is

$$V = N . \tag{29}$$

The polyhedron will have F faces, each of which will have associated with it a value of $v_f (f = 1, 2, \ldots, F)$, where v_f is the largest value of γ that can exist for the three points defining the triangle. The largest of the values v_f is then v_m. By Euler's theorem,

$$F - E + V = 2 \quad , \tag{30}$$

where E is the number of edges. Each face has three edges but each edge is shared by two faces. Hence,

$$E = \frac{3}{2} F \quad . \tag{31}$$

By substituting Eq. (29) and Eq. (31) into Eq. (30), one obtains

$$F = 2N - 4 \tag{32}$$

and

$$E = 3N - 6 \quad . \tag{33}$$

If all the triangles can be made equilateral and congruent, it can be demonstrated that the smallest value of v_m possible will result. Although there are only three polyhedra where this is possible (tetrahedron N = 4, octahedron N = 6, and icosahedron N = 12), such a device is useful for any value of N because it permits one to obtain a hypothetical value of v_m, say G, which is known to be smaller than the best possible value. If we have a geometry that has a value of v_m very close to the value of G, then the geometry must be very nearly optimum.

To prove that the hypothetical geometry is better than the optimum, we shall assume that a better geometry than the hypothetical one exists and we shall show that an impossible situation follows. For the assumed geometry, all the values of v_f would be less than the value G. It will be shown below that for any value v_f, the triangle on the spherical surface with the largest area is equilateral. Since each triangle of the hypothetical geometry is also equilateral and $v_f < G$, then

$$A_f < \frac{4\pi}{F} \quad ,$$

where A_f and $4\pi/F$ are, respectively, the areas of a face of the assumed geometry and a face of the hypothetical geometry. Also, it is necessary that

$$\sum_{f=1}^{F} A_f = 4\pi \quad .$$

Hence,

$$\sum_{f=1}^{F} \frac{4\pi}{F} < 4\pi \quad ,$$

and since each term of the series is the same, then

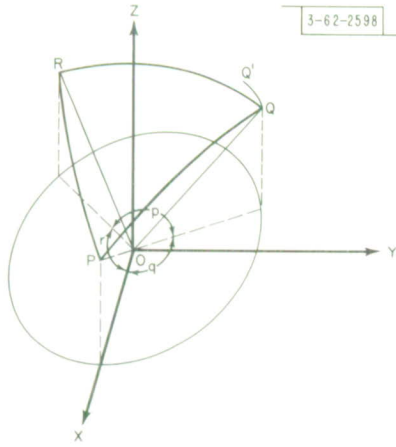$$F(\frac{4\pi}{F}) < 4\pi \quad ,$$

which is impossible.

3-62-2598

Fig. 5. Geometry showing the spherical triangle formed by three adjacent antenna pointing directions OP, OQ, and OR.

Consider one of the spherical triangles, say PQR, in a coordinate system, as shown in Fig. 5. This triangle is oriented so that direction OP is in the X-Z plane and angles $POZ° = QOZ° = ROZ° = \gamma$. Also, let the angles separating the planes containing the Z-axis and points P, Q, and R, be p, q, and r, as shown. Hence,

$$p + q + r = 2\pi \quad , \tag{34}$$

and the coordinates are

$$P(\sin\gamma, \ 0, \ \cos\gamma) \quad ,$$

$$Q(\sin\gamma\cos q, \ \sin\gamma\sin q, \ \cos\gamma) \quad ,$$

and

$$R(\sin\gamma\cos r, \ -\sin\gamma\sin r, \ \cos\gamma) \quad .$$

If angles q and r have values where the area of triangle PQR is maximum, then any infinitesimal change in q or r will produce no change in area. That is, if angle q increases by dq, point Q moves to Q' and the change in area is 0, or

$$\Delta RQQ' - \Delta PQQ' = 0 \quad . \tag{35}$$

Now $\Delta PQQ'$ must be proportional to dq to the first order and must be a function of q and γ alone. Hence,

$$\Delta PQQ' = f(q,\gamma) \ dq \quad . \tag{36}$$

Similarly,

$$\Delta RQQ' = f(p,\gamma) \ (-dp) \quad , \tag{37}$$

where the same function f is used but with p replacing q. Since dq = −dp, one finds that

$$f(q,\gamma) = f(p,\gamma) \quad . \tag{38}$$

Similarly, a change in area due to an increase in angle r is also 0 and

$$f(r,\gamma) = f(p,\gamma) \quad . \tag{39}$$

Certainly, one solution of Eqs. (34), (38), and (39) is

$$p = q = r = \frac{2}{3}\pi = 120° \quad . \tag{40}$$

If the function f is actually evaluated and Eq. (38) is solved, one gets the result

$$q = p + n\pi \quad , \qquad n = 0, \pm 1, \pm 2, \dots \quad .$$

However, for values of n other than 0, the area is smaller. Hence, the triangle with the largest area is equilateral.

For the hypothetical geometry, $\gamma = G$, $q = 2\pi/3$, and $r = 2\pi/3$, and the coordinates become

$$P(\sin G, \ 0, \ \cos G) \quad ,$$

$$Q\left(-\frac{1}{2} \sin G, \ \frac{\sqrt{3}}{2} \sin G, \ \cos G\right) \quad ,$$

and

$$R\left(-\frac{1}{2} \sin G, \ -\frac{\sqrt{3}}{2} \sin G, \ \cos G\right) \quad .$$

The plane containing the points P, Q, and O has equation

$$x \cos G + y \sqrt{3} \cos G - z \sin G = 0 \quad , \tag{41}$$

and its normal is

$$\vec{N} = \vec{i} \cos G + \vec{j} \sqrt{3} \cos G - \vec{k} \sin G \quad . \tag{42}$$

The spherical angle QPR° is double the angle between $\vec{N}$ and the Y-axis and is given by

$$\cos \frac{QPR°}{2} = \frac{\vec{N} \cdot \vec{j}}{|\vec{N}|} \quad . \tag{43}$$

By substituting Eq. (42) into Eq. (43) and solving for G, one obtains

$$\cos G = \frac{1}{\sqrt{3}} \cot \frac{QPR°}{2} \quad . \tag{44}$$

Since several lines radiate from point P to delineate a corresponding number of triangles all with angle QPR°, there must be $2\pi/QPR°$ lines meeting at each point P. Referring again to the picture of the polyhedron, we see that there are $2\pi/QPR°$ edges meeting at each vertex and that since each edge is shared by 2 vertices, the total number of edges is

$$E = \frac{\pi N}{QPR°} \quad . \tag{45}$$

From Eqs. (33) and (45), one obtains

$$QPR° = \frac{\pi}{3} \frac{N}{N - 2} \quad , \tag{46}$$

and from Eq. (44)

$$\cos G = \frac{1}{\sqrt{3}} \cot \frac{\pi}{6} \frac{N}{N - 2} \quad . \tag{47}$$

This formula provides a useful method of indicating how good the geometry is that we choose to investigate, by permitting a comparison of the value of v_m with that of G. An incidental outcome of this theory is that the area of one of the spherical triangles can be derived in terms of angle QPR° by equating the area to $4\pi/F$ and substituting for F [Eq. (32)] and then for N [Eq. (46)]. The result obtained agrees with that educed in spherical trigonometry, as it should.

11

Now we can proceed to choose pointing direction geometries and investigate their character-
istics for the various values of N. The values chosen, mainly for their ease of solution, are
N = 4, 6, 8, 12, 16, 24, 32, 48, and 60. In each case, the positions of the points are chosen in
order to have the largest number of triangles equilateral and the values of v_f at or near v_m.
There is no evidence that the choices are the best, but the comparisons of the values v_m with
G show them to be good. The choices are based largely on the geometries given in the paper of
Schütte and van der Waerden.[*] In the case N = 32, two geometries are given. One has slightly
poorer characteristics but its geometry repeats in the 8 octants which may be more convenient
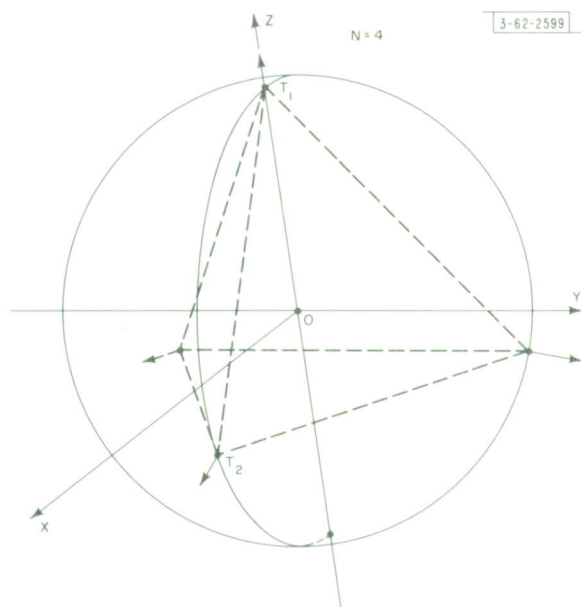for some applications.

Fig. 6. Geometry showing the chosen pointing
directions for 4 antennas.

N = 4 (Fig. 6)

The 4 points are at the vertices of a tetrahedron.

Geometry symmetries:

All triangles are equilateral and congruent.

Coordinates:

T_1 (0, 0, 1.00000)

T_2 (0.94281, 0, −0.33333), etc.

v_m = G = 70.53°

A plot of P(α < a) for this geometry is shown in Fig. 7.

[*] K. Schütte and B.L. van der Waerden, "Auf welcher Kugel haben 5, 6, 7, 8 oder 9 Punkte mit Mindestabstand
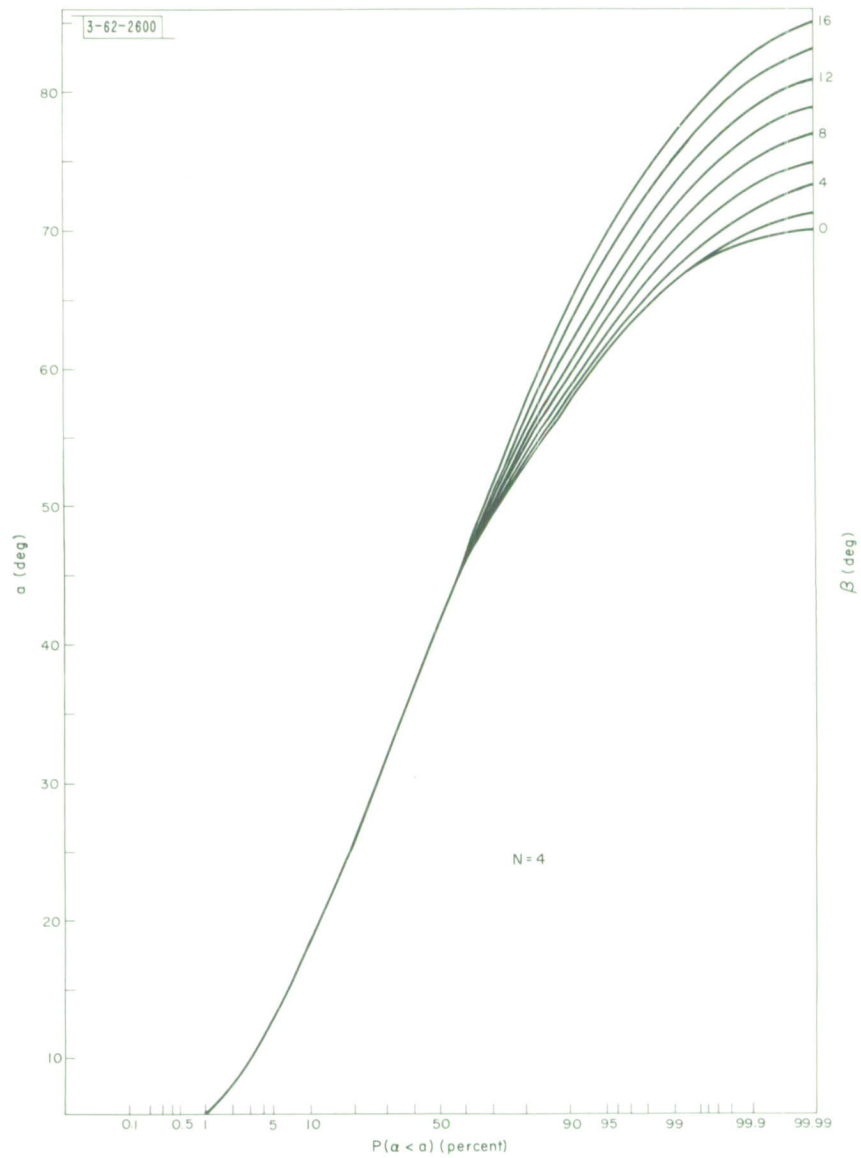Eins Platz?" Math. Annalen 123, 96 (1951).

Fig. 7. Probability that receiver is at an angle less than a from the pointing direction of the antenna in operation for the 4-antenna geometry (Fig. 6).
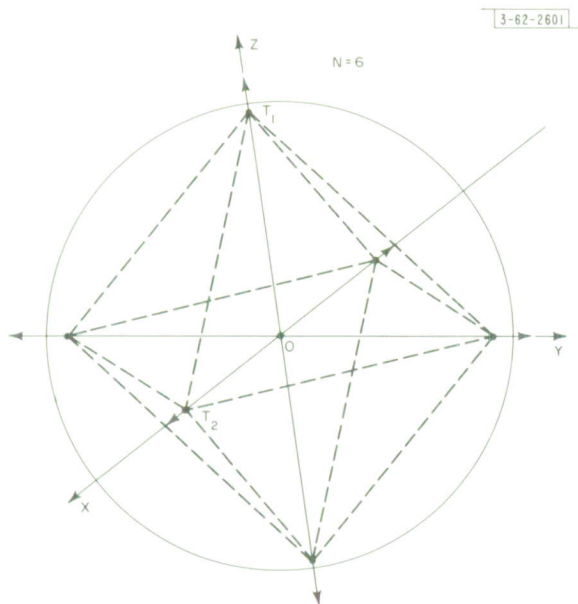
13

Fig. 8. Geometry showing the chosen pointing directions for 6 antennas.

N = 6 (Fig. 8)

The 6 points are at the vertices of an octahedron.

Geometry symmetries:

All triangles are equilateral and congruent.

Coordinates:

T_1 (0, 0, 1.00000)

T_2 (1.00000, 0, 0), etc.

$v_m = G = 54.74°$.

A plot of $P(\alpha < a)$ for this geometry is shown in Fig. 9.

N = 8 (Fig. 10)

4 points are midway between the X-Z and Y-Z planes and lie above the X-Y plane.

4 points are on the X-Z and Y-Z planes and lie below the X-Y plane.

All points are the same distance from the X-Y plane.

Introduce points U_1 on Z-axis, U_2 on X-Z plane and U_3 on negative Z-axis.

Condition:

$T_1 U_1 = T_1 U_2 = T_5 U_2 = T_5 U_3$.

Geometry symmetries:

4 triangles (e.g., $T_1 T_2 T_3$) are right angle, isosceles and congruent and $v_f = v_m$.

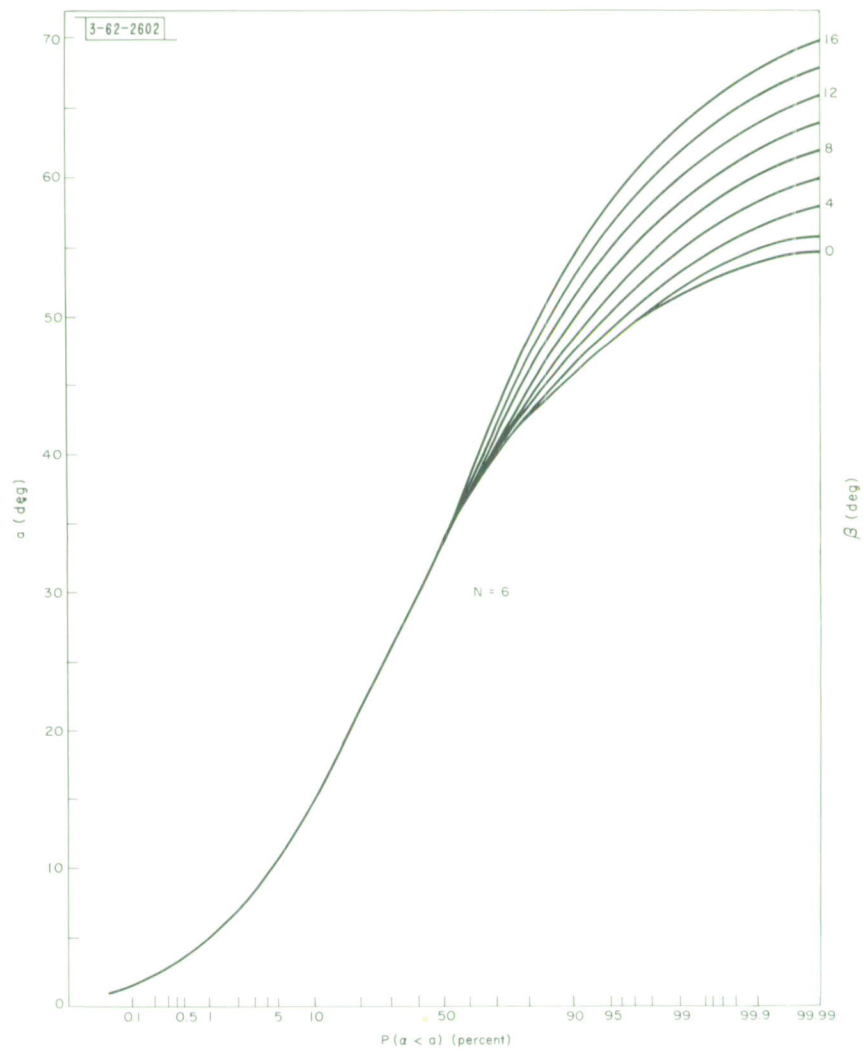8 triangles (e.g., $T_1 T_2 T_6$) are isosceles and congruent and $v_f = v_m$.

14

Fig. 9. Probability that receiver is at an angle less than a from the pointing direction of the antenna in operation for the 6-antenna geometry (Fig. 8).
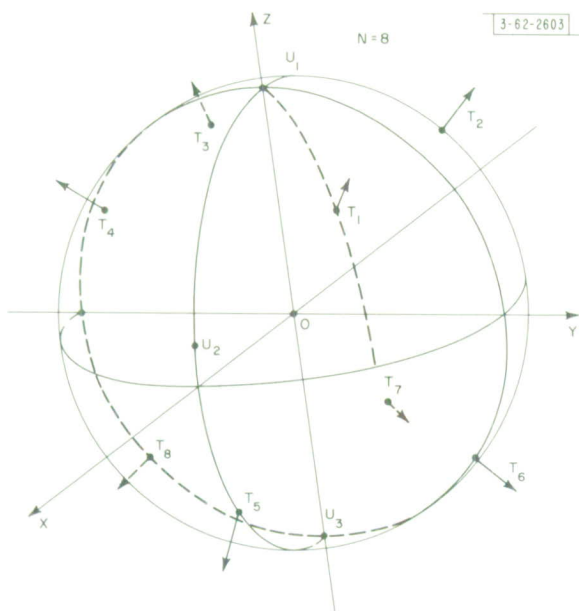
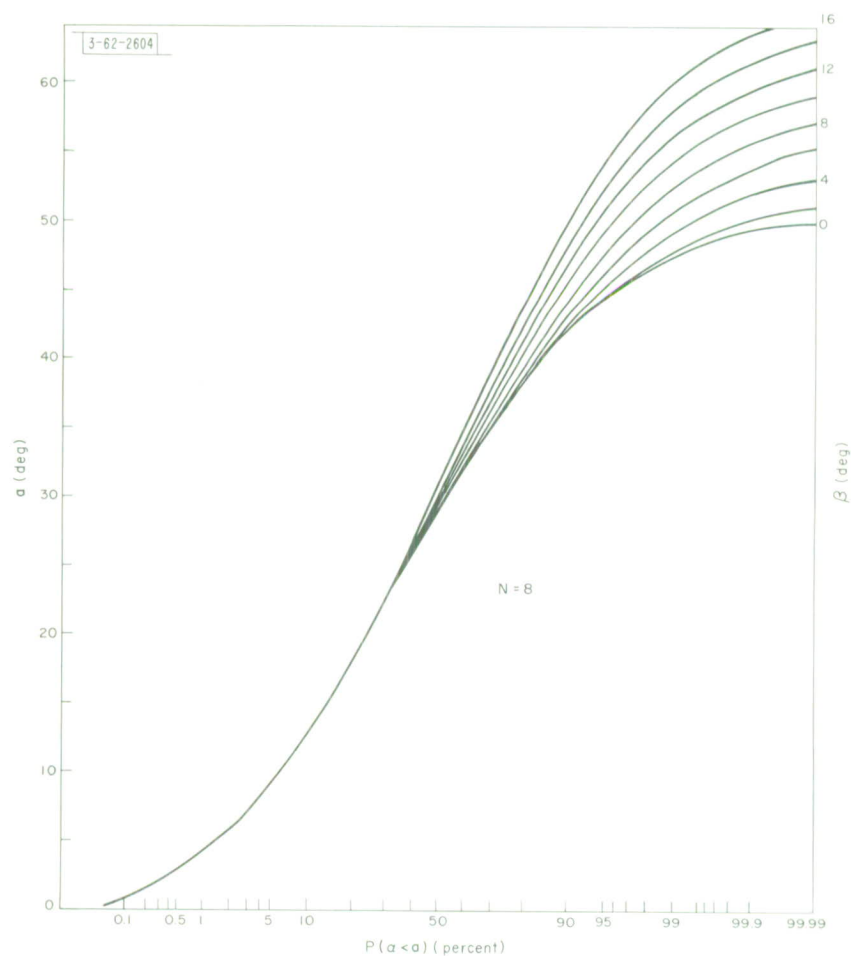Fig. 10. Geometry showing the chosen pointing directions for 8 antennas.

Fig. 11. Probability that receiver is at an angle less than a from the pointing direction of the antenna in operation for the 8-antenna geometry (Fig. 10).

Coordinates:

T_1 (0.54120, 0.54120, 0.64359)

T_5 (0.76537, 0, −0.64359), etc.

U_2 (0.98517, 0, 0.17157)

$v_m = 49.94°$

$G = 46.52°$.

A plot of $P(\alpha < a)$ for this geometry is shown in Fig. 11.

N = 12 (Fig. 12)

The 12 points are at the vertices of an icosahedron.

Geometry symmetries:

All triangles are equilateral and congruent.

Coordinates:

T_1 (0, 0, 1.00000)

T_2 (0.89443, 0, 0.44721)

T_3 (0.27639, 0.85065, 0.44721)

T_4 (0.72361, 0.52573, −0.44721), etc.

$v_m = G = 37.38°$.

A plot of $P(\alpha < a)$ for this geometry is shown in Fig. 13.

N = 16 (Fig. 14)

4 points are on the X-Z and Y-Z planes and lie above the X-Y plane.

4 points are midway between the X-Z and Y-Z planes and lie below the X-Y plane.

The 8 points are the same distance from the X-Y plane.

4 points are midway between the X-Z and Y-Z planes and lie above the X-Y plane.

4 points are on the X-Z and Y-Z planes and lie below the X-Y plane.

The 8 points are the same distance from the X-Y plane.

Introduce points U_1 on Z-axis, U_2 midway between X-Z and Y-Z planes and U_3.

Condition:

$T_1U_1 = T_1U_2 = T_1U_3 = T_3U_2 = T_3U_3 = T_4U_3$.

Geometry symmetries:

4 triangles (e.g., $T_1T_2T_5$) are right angle, isosceles and congruent and $v_f = v_m$.

8 triangles (e.g., $T_1T_2T_3$) are isosceles and congruent and $v_f = v_m$.

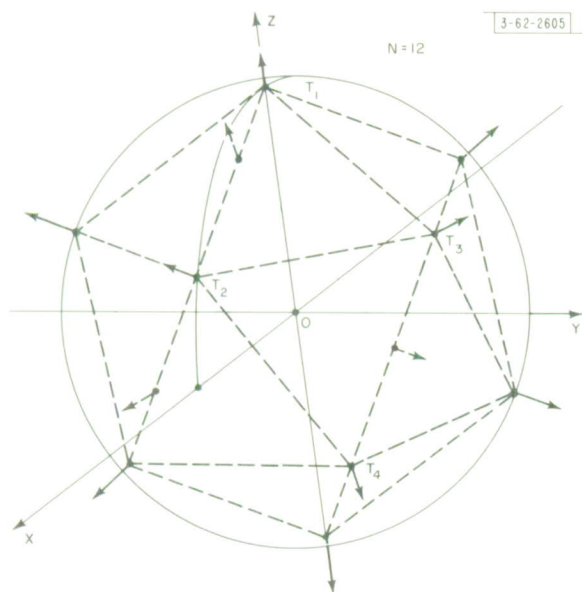16 triangles (e.g., $T_1T_3T_4$) are congruent and $v_f = v_m$.

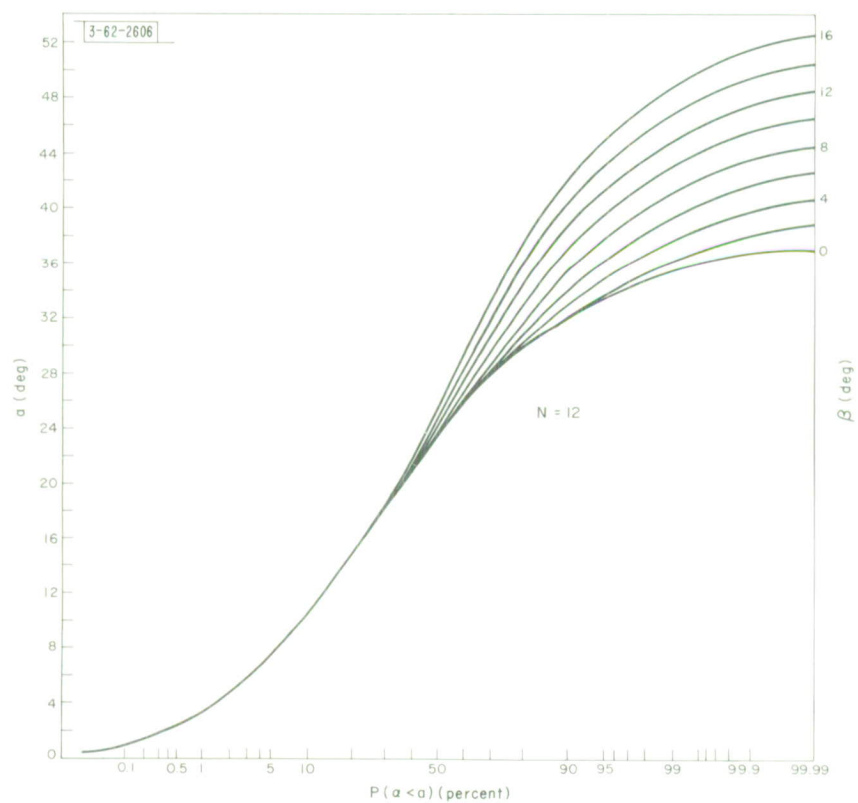Fig. 12. Geometry showing the chosen pointing directions for 12 antennas.

Fig. 13. Probability that receiver is at an angle less than a from the pointing direction of the antenna in operation for the 12-antenna geometry (Fig. 12).

18

Coordinates:

T_1 (0.55598, 0, 0.83119)

T_4 (0.99524, 0, −0.09749)

T_3 (0.70374, 0.70374, 0.09749), etc.

U_2 (0.54661, 0.54661, 0.63437)

U_3 (0.87575, 0.24798, 0.41421)

v_m = 33.78°

G = 32.13°.

A plot of $P(\alpha < a)$ for this geometry is shown in Fig. 15.

N = 24 (Fig. 16)

3 points are in each octant which form an equilateral triangle centered in the octant.

The geometry is the same for all octants.

Introduce points U_1 on Z-axis, U_2 at the midpoint of the first octant and U_3.

Conditions:

$T_1T_2 = T_2T_3 = T_1T_3$.

$T_1U_1 = T_1U_2 = T_2U_2 = T_3U_2 = T_1U_3 = T_2U_3 = T_4U_3$.

Geometry symmetries:

12 triangles (e.g., $T_1T_4T_5$) are right angle, isosceles and congruent and $v_f = v_m$.

8 triangles (e.g., $T_1T_2T_3$) are equilateral and congruent and $v_f = v_m$.

24 triangles (e.g., $T_1T_2T_4$) are congruent and $v_f = v_m$.

Coordinates:

T_1 (0.26993, 0.37827, 0.88546)

T_2 (0.88546, 0.26993, 0.37827), etc.

U_2 (0.57735, 0.57735, 0.57735)

U_3 (0.64344, 0.10754, 0.75791)

v_m = 27.69°

G = 26.05°.

A plot of $P(\alpha < a)$ for this geometry is shown in Fig. 17.

N = 32, Case 1 (Fig. 18)

8 points are at the midpoints of the octants.

24 points lie on the coordinate planes at equal distances from the axes.

The geometry is the same for all octants.

Introduce points U_1 on Z-axis and U_2 midway between X-Y and Y-Z plane.

3-62-2607

N = 16

Fig. 14. Geometry showing the chosen pointing directions for 16 antennas.

3-62-2608

N = 16

$P(\alpha < a)$ (percent)

a (deg)

β (deg)

Fig. 15. Probability that receiver is at an angle less than a from the pointing direction of the antenna in operation for the 16-antenna geometry (Fig. 14).

3-62-2609   N = 24

Fig. 16. Geometry showing the chosen pointing directions for 24 antennas.

3-62-2610

N = 24

$P(a < a)$ (percent)

Fig. 17. Probability that receiver is at an angle less than a from the pointing direction of the antenna in operation for the 24-antenna geometry (Fig. 16).

21
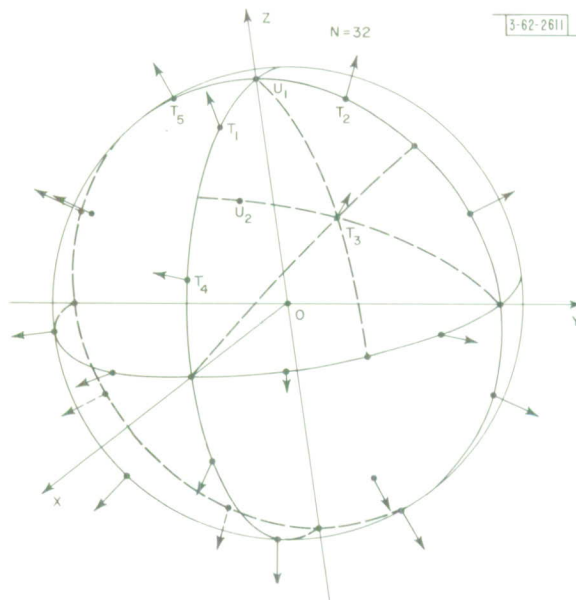
Fig. 18. Geometry for one set of pointing directions for 32 antennas.
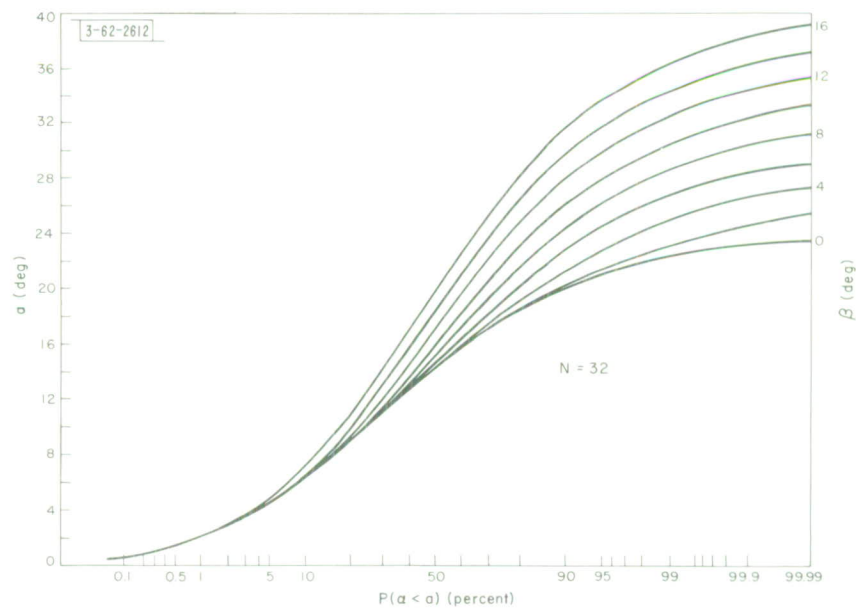
Fig. 19. Probability that receiver is at an angle less than α from the pointing direction of the antenna in operation for the 32-antenna geometry (Fig. 18).

Condition:

$$T_1U_1 = T_1U_2 = T_3U_2.$$

Geometry symmetries:

12 triangles (e.g., $T_1T_2T_5$) are right angle, isosceles and congruent and $v_f = v_m$.

24 triangles (e.g., $T_1T_3T_4$) are isosceles and congruent and $v_f = v_m$.

24 triangles (e.g., $T_1T_2T_3$) are isosceles and congruent and $v_f < v_m$.

Coordinates:

T_1 (0.40475, 0, 0.91443)

T_3 (0.57735, 0.57735, 0.57735)

T_4 (0.91443, 0, 0.40475), etc.

U_2 (0.69318, 0.19747, 0.69318)

$v_m = 23.88°$

$G = 22.49°$.

A plot of $P(\alpha < a)$ for this geometry is shown in Fig. 19.

N = 32, Case 2 (Fig. 20)

12 points are at the vertices of an icosahedron.

20 points are at the midpoints of the triangles of the icosahedron.

Geometry symmetries:

All triangles are isosceles and congruent.
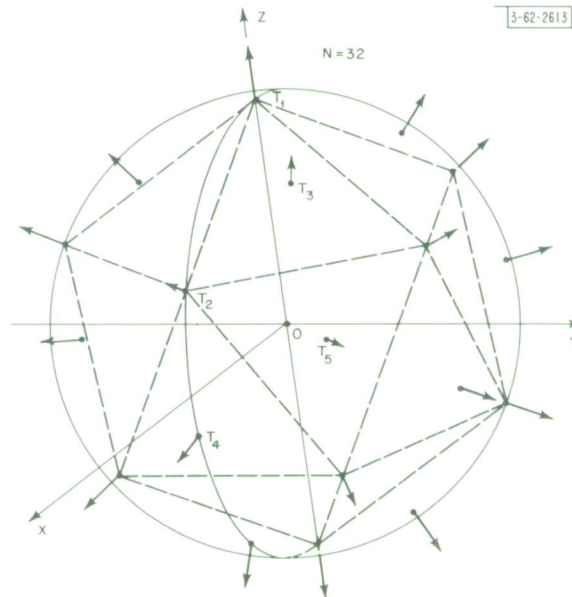
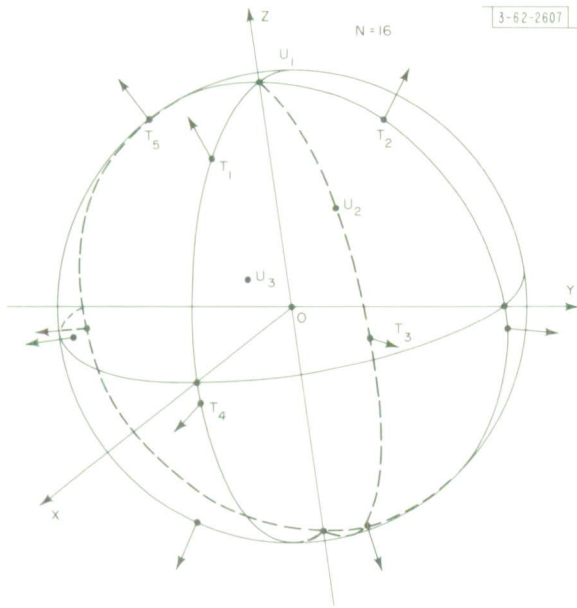Fig. 20. Geometry for a second set of pointing directions for 32 antennas.

Fig. 21. Geometry showing the chosen pointing directions for 48 antennas.
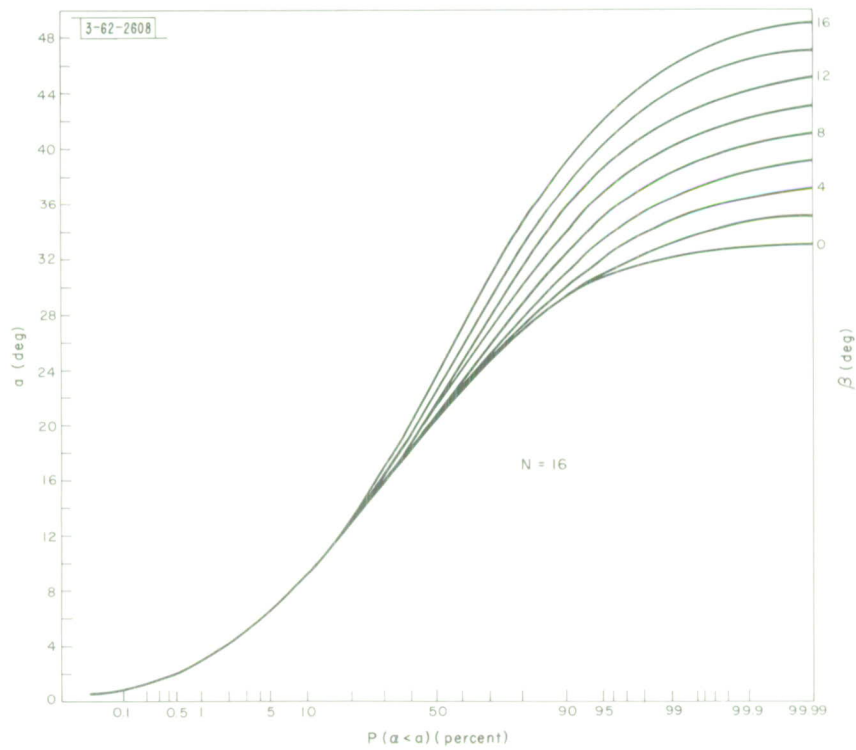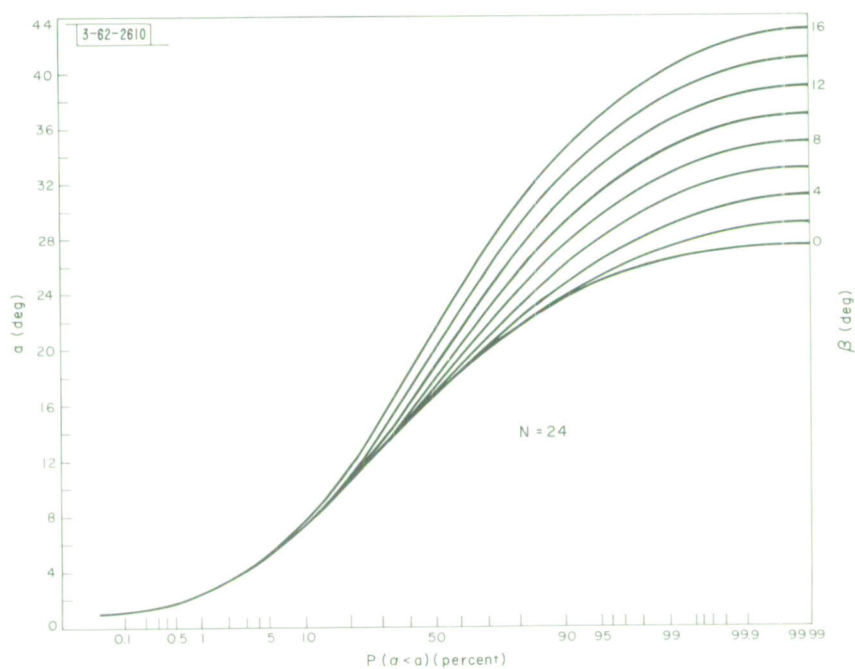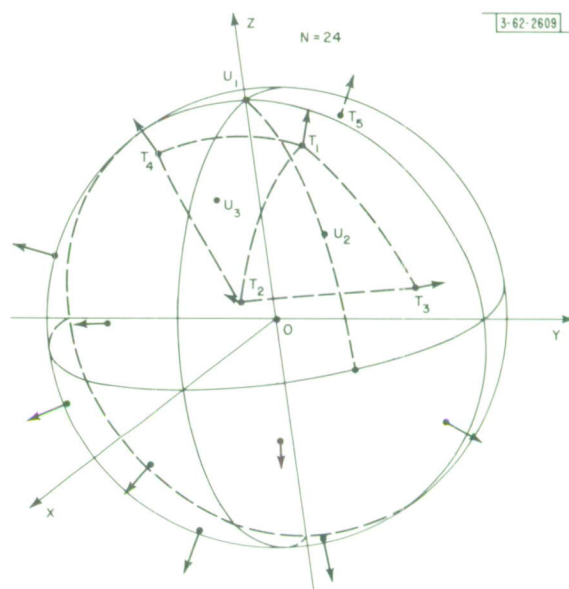

Fig. 22. Probability that receiver is at an angle less than α from the pointing direction of the antenna in operation for the 48-antenna geometry (Fig. 21).

24

Coordinates:

> T_1 (0, 0, 1.00000)
>
> T_2 (0.89443, 0, 0.44721)
>
> T_3 (0.49112, 0.35682, 0.79465)
>
> T_4 (0.98225, 0, −0.18759)
>
> T_5 (0.79465, 0.57735, 0.18759), etc.

$v_m = 22.69°$

$G = 22.49°$.

N = 48 (Fig. 21)

6 points are in each octant which form a cluster of 4 equilateral triangles centered in the octant.

The geometry is the same for all octants.

Introduce points U_1 on Z-axis, U_2 at midpoint of an octant and U_3.

Conditions:

> $T_1T_2 = T_2T_3 = T_1T_3 = T_2T_4 = T_2T_5 = T_4T_5 = T_3T_5 = T_3T_6 = T_5T_6$.
>
> $T_1U_1 = T_2U_2 = T_3U_2 = T_5U_2 = T_2U_3 = T_7U_3 = T_8U_3$.

Geometry symmetries:

> 12 triangles (e.g., $T_1T_7T_9$) are right angle, isosceles and congruent and $v_f = v_m$.
>
> 32 triangles (e.g., $T_1T_2T_3$) are equilateral and congruent and $v_f = v_m$.
>
> 24 triangles (e.g., $T_2T_7T_8$) are congruent and $v_f = v_m$.
>
> 24 triangles (e.g., $T_1T_2T_7$) are congruent and $v_f < v_m$.

Coordinates:

> T_1 (0.09252, 0.31372, 0.94500)
>
> T_4 (0.94500, 0.09252, 0.31372)
>
> T_2 (0.61706, 0.28702, 0.73270)
>
> T_5 (0.73270, 0.61706, 0.28702), etc.
>
> U_2 (0.57735, 0.57735, 0.57735)
>
> U_3 (0.60477, −0.03842, 0.79547)

$v_m = 19.09°$

$G = 18.30°$.

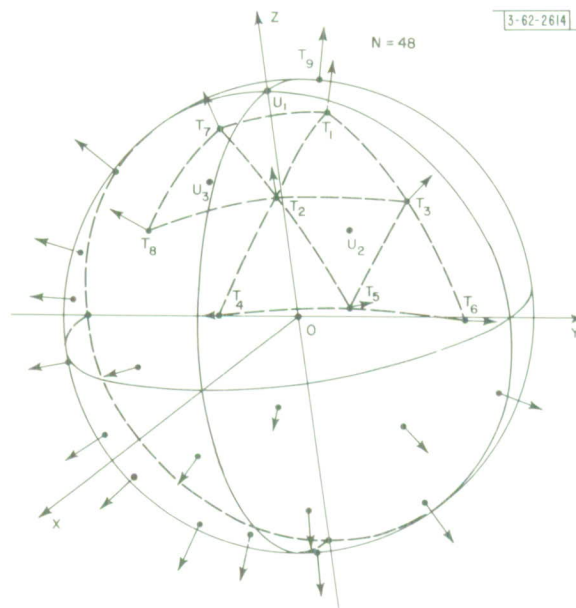A plot of $P(\alpha < a)$ for this geometry is shown in Fig. 22.

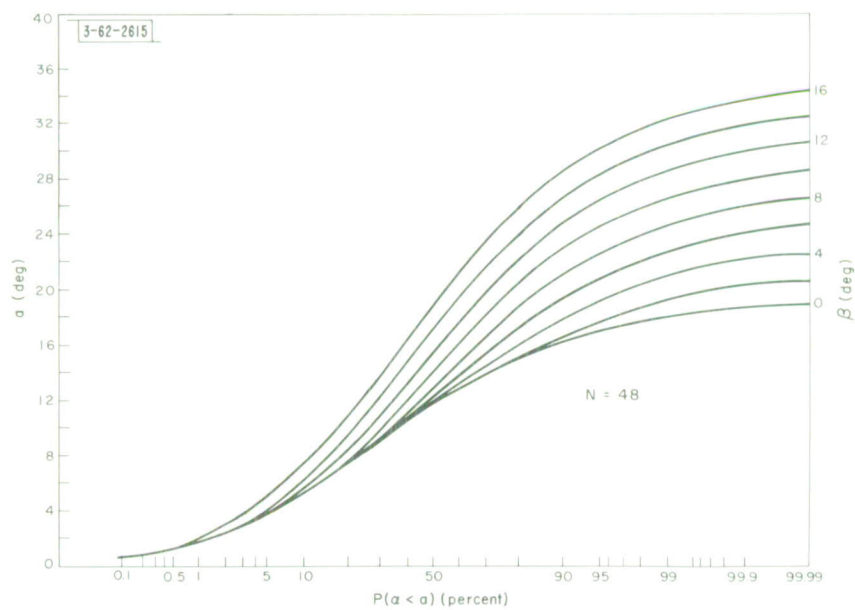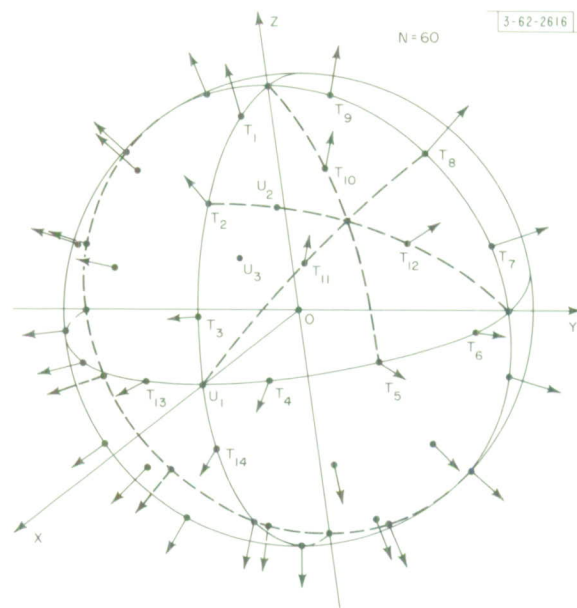Fig. 23. Geometry showing the chosen pointing directions for 60 antennas.
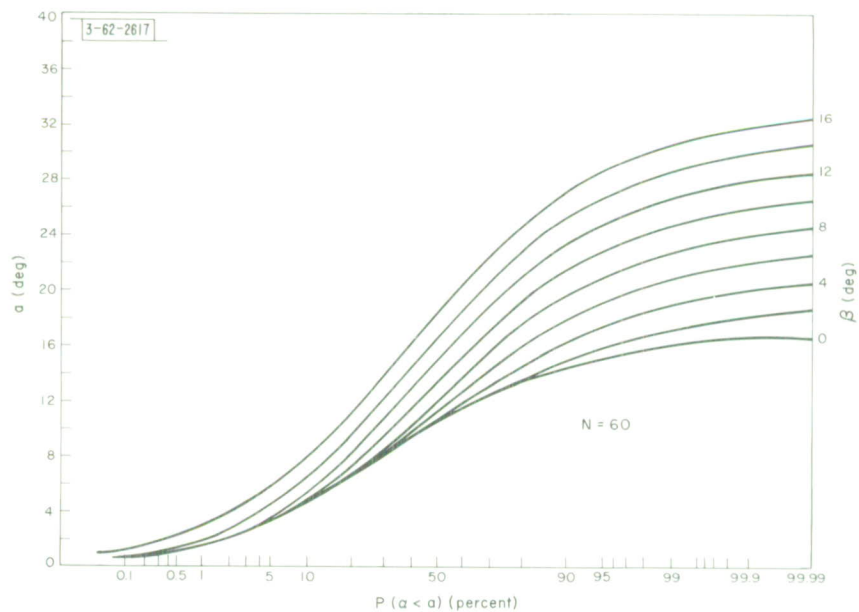
Fig. 24. Probability that receiver is at an angle less than a from the pointing direction of the antenna in operation for the 60-antenna geometry (Fig. 23).

N = 60 (Fig. 23)

36 points lie on the coordinate planes.

24 of the 36 points are the same distance from the axes.

The other 12 are midway between 2 axes.

24 points are midway between two coordinate planes at equal distances from the centers of the octants.

The geometry is the same for all octants.

Introduce points U_1 on X-axis, U_2 midway between X-Y and Y-Z planes and U_3.

Condition:

$$T_3U_1 = T_3U_3 = T_2U_3 = T_{11}U_3 = T_2U_2 = T_{11}U_2.$$

Geometry symmetries:

12 triangles (e.g., $T_3T_4T_{13}$) are right angle, isosceles and congruent and $v_f = v_m$.

24 triangles (e.g., $T_3T_4T_{11}$) are isosceles and congruent and $v_f < v_m$.

48 triangles (e.g., $T_2T_3T_{11}$) are congruent and $v_f = v_m$.

24 triangles (e.g., $T_2T_{10}T_{11}$) are isosceles and congruent and $v_f = v_m$.

8 triangles (e.g., $T_{10}T_{11}T_{12}$) are equilateral and congruent and $v_f < v_m$.

Coordinates:

T_3 (0.95660, 0, 0.29140)

T_2 (0.70711, 0, 0.70711)

T_{11} (0.77565, 0.44630, 0.44630), etc.

U_2 (0.67642, 0.29140, 0.67642)

U_3 (0.84544, 0.16667, 0.50740)

$v_m = 16.94°$

$G = 16.35°.$

A plot of $P(\alpha < a)$ for this geometry is shown in Fig. 24.

V. INCLUSION OF ANTENNA PATTERN CHARACTERISTICS

Having determined the probability distribution of angle α for a specific geometry, one will want to design an antenna whose pattern is most suitable for the case of interest. As an example, suppose we want to build a satellite with 32 antennas arranged as shown in Fig. 18, which is to have an RF power source strong enough to allow messages to be received 100 percent of the time at stations located anywhere where β is 8° or less. Referring to Fig. 19, we see that angle α will have values up to a = 31.9°. The antenna is designed for maximum gain at this angle, thus minimizing the power requirements of the RF source. If reception for 80 percent of the time were allowed, angle α would be less than a = 21.6° for 80 percent of the time, and the antennas could be designed for maximum gain at 21.6° which would be higher than the gain of the first

antenna. Similarly, smaller values of β would permit smaller values of a and correspondingly higher antenna gains for the same probability.

To illustrate better the application of the antenna pattern, suppose the pattern is given by

$$g = \frac{2J_1(g_0 \sin \alpha)}{\sin \alpha} \quad , \tag{48}$$

where J_1 is the Bessel function of the first kind, g is the signal amplitude at angle α off the axis, and g_0 is the signal amplitude on the axis ($\alpha = 0$). This pattern is based on the situation where a plane wavefront emanates from a circular aperture and it is fairly representative of RF horns in general. The antenna designer has a choice of the value g_0 at his disposal. It is approximately

$$g_0 = \frac{2\pi r}{\lambda} \quad , \tag{49}$$

where r is the aperture radius.

The half-power beamwidth HPBW is found by Eq. (48), where

$$\alpha = \frac{1}{2} \text{ HPBW} \tag{50}$$

and

$$g = \frac{g_0}{\sqrt{2}} \quad . \tag{51}$$
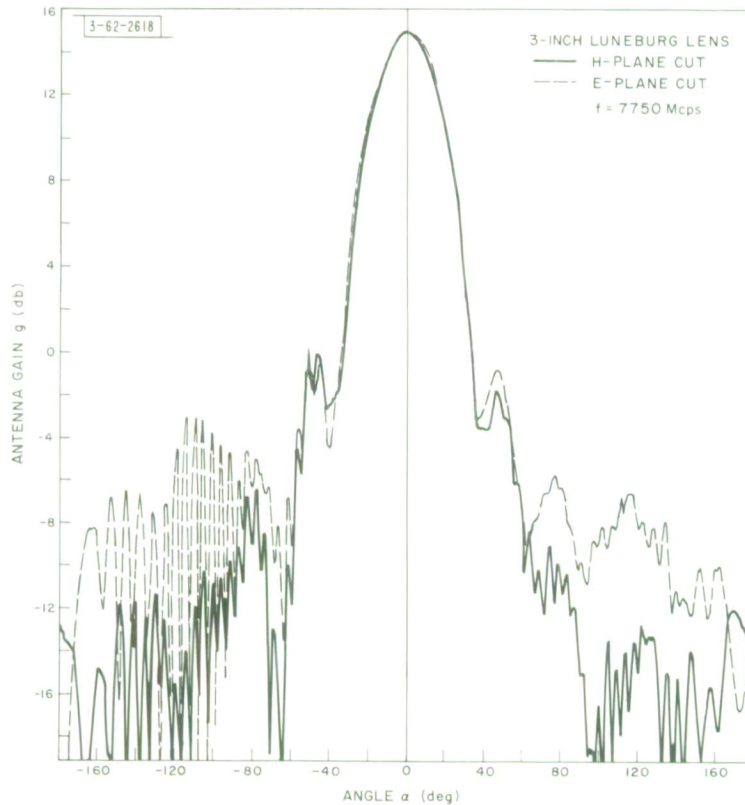
Fig. 25. Pattern of a circular pipe of 1-inch aperture butted against a Luneburg lens of 3-inch diameter taken at a frequency of 7750 Mcps.

Hence,

$$g_O \sin \frac{1}{2} \text{HPBW} = 1.616 \tag{52}$$

or

$$\text{HPBW} = 2 \sin^{-1}\left(\frac{1.616}{g_O}\right) \quad . \tag{53}$$

Now at $\alpha = a$, gain g is maximum when g_O has a value where J_1 is maximum. The values are, from Eq. (48),

$$g_O \sin a = 1.841 \tag{54}$$

and

$$g \sin a = 1.164 \quad . \tag{55}$$

An immediate observation is that

$$\frac{g}{g_O} = 0.632 \to -3.98 \, \text{db} \quad , \tag{56}$$

and the maximum range of gain values is 3.98 db for the optimum pattern. In our example, where $a = 31.9°$, $g_O = 3.486 \to 10.85$ db, and $g = 2.204 \to 6.87$ db.

A similar analysis was applied to the other geometries and the results are summarized in Appendix A. Two values of β, 0° and 8°, were considered. The trends in a change of N or β are easily noted and for values not included, the characteristics can be estimated.

It is useful to give an example of the application of an actual pattern to a probability distribution. The pattern shown in Fig. 25 (very nearly the same in the E- or H-plane) is of a circular pipe of 1-inch aperture butted against a Luneburg lens of 3-inch diameter taken at a frequency of 7750 Mcps. For this pattern, HPBW = 34° and $g_O = 5.69 \to 15.1$ db, and hence $g_O \sin \frac{1}{2} \text{HPBW} = 1.66$, which agrees well with the value given by Eq. (52). This pattern, in conjunction with the geometry of Fig. 18, produces a probability distribution as shown in Fig. 26. These curves were
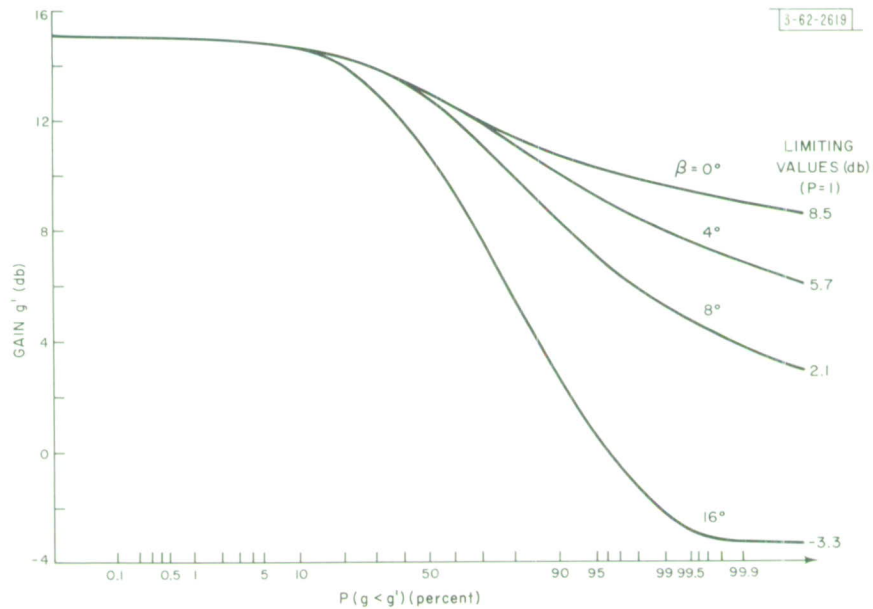
Fig. 26. Probability that the antenna gain is less than a value g' in the direction of the receiver for the geometry of Fig. 18 using the pattern in Fig. 25.
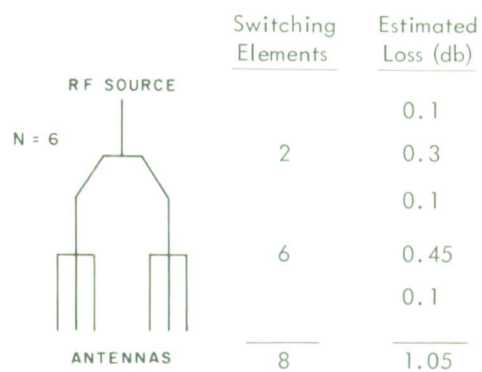
29

(a) 4-antenna system.

	Switching Elements	Estimated Loss (db)
N = 4		0.1
	4	0.6
		0.1
	4	0.8

(b) 6-antenna system.

	Switching Elements	Estimated Loss (db)
N = 6		0.1
	2	0.3
		0.1
	6	0.45
		0.1
	8	1.05

(c) 8-antenna system.

	Switching Elements	Estimated Loss (db)
N = 8		0.1
	2	0.3
		0.1
	8	0.6
		0.1
	10	1.2

(d) 12-antenna system.

	Switching Elements	Estimated Loss (db)
N = 12		0.1
	3	0.45
		0.1
	12	0.6
		0.1
	15	1.35

(e) 16-antenna system.

	Switching Elements	Estimated Loss (db)
N = 16		0.1
	4	0.6
		0.1
	16	0.6
		0.1
	20	1.5
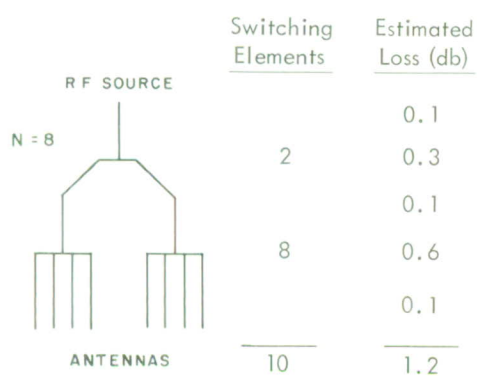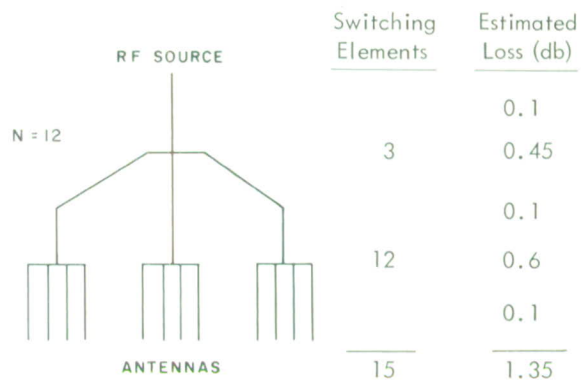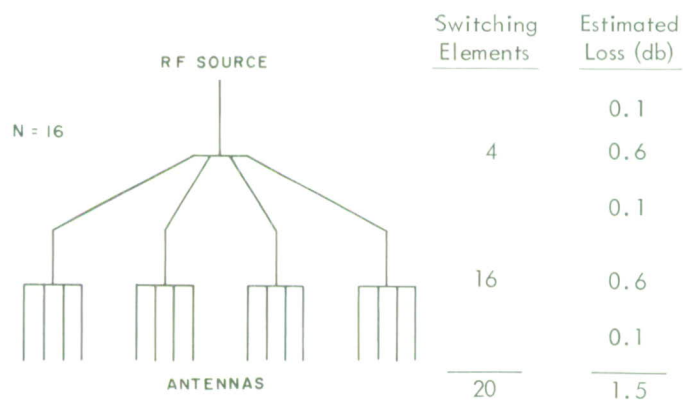
Fig. 27(a-i). Switching matrix and estimated insertion loss for various values of N.

simply obtained by converting the angles a of Fig. 19 to gains by Fig. 25. The choice of pattern for this geometry is not optimum, and where the gains may drop to say 8.5 db for $\beta = 0°$ or 2.1 db for $\beta = 8°$, the gains would drop at the most to 9.2 and 6.9 db, respectively, if the optimum patterns were used.

The ideal antenna for this application is one where the gain is constant for angle α less than a and 0 otherwise (within the restriction of retaining circular symmetry). Then

$$g_{ideal} = \frac{1}{\sin \frac{a}{2}} \quad , \quad \alpha < a \tag{57a}$$

or

$$g_{ideal} = 0 \quad , \quad \alpha > a \quad . \tag{57b}$$

On comparison with the gain given by Eq. (55),

$$\frac{g_{ideal}}{g} = \frac{\cos \frac{a}{2}}{0.582} \quad . \tag{58}$$

Approximately, $\cos a/2 = 1$ and the ratio is 4.7 db. If such a pattern could be created, the RF power necessary for communication is correspondingly reduced. However, the opportunities for shaping a more desirable pattern are impeded by the difficulties of maintaining a simple antenna design.

VI. CONSIDERATION OF THE RF CIRCUITS

To complete this study, some consideration should be given to the switching matrix supplying the RF to the appropriate antenna. The matrix will be assumed to contain switches that are either SP2T, SP3T or SP4T. The expected switching matrices for the various values of N are shown in Fig. 27(a-i). If we assume that there is an insertion loss of 0.6 db in a SP4T switch, 0.45 db in a SP3T switch, 0.3 db in a SP2T switch and 0.1 db in each length of transmission line connecting the switches to each other, to the power source or to the antennas, we can estimate the total loss of RF through the matrix. The results are given in Appendix A. (The values of switch insertion losses are based on experimental evidence obtained for switches using PIN diodes in waveguide packages, where f = 7750 Mcps. Ferrites should show better characteristics but they are less desirable for satellite applications due to weight and driving power requirements.)

Each SP2T, SP3T or SP4T switch requires 2, 3 or 4 switching elements. For example, for the matrix of 32 antennas, 42 switching elements are needed. One can appreciate the complexity of the logic circuits and the problems of generating power to operate switching elements, if the number of antennas is large.

VII. CONCLUSIONS

The results of this study are well summarized in Appendix A. The choice of the number of antennas will also depend on factors other than those mentioned in this report. However, it appears that for the small reduction in RF power requirements, more than 12 or 16 antennas are not warranted, due to the complexity of the switching circuits. A fair appraisal should also include a comparison of this type of satellite with one that does not contain switches but is designed to radiate as close to isotropic as possible. In any case, this system is put forth as a preferable means, for some types of communication, of linking two distant locations on the earth.

	Switching Elements	Estimated Loss (db)
N = 24		0.1
	2	0.3
		0.1
	6	0.45
		0.1
	24	0.6
		0.1
	32	1.75

(f) 24-antenna system.

	Switching Elements	Estimated Loss (db)
N = 32		0.1
	2	0.3
		0.1
	8	0.6
		0.1
	32	0.6
		0.1
	42	1.9
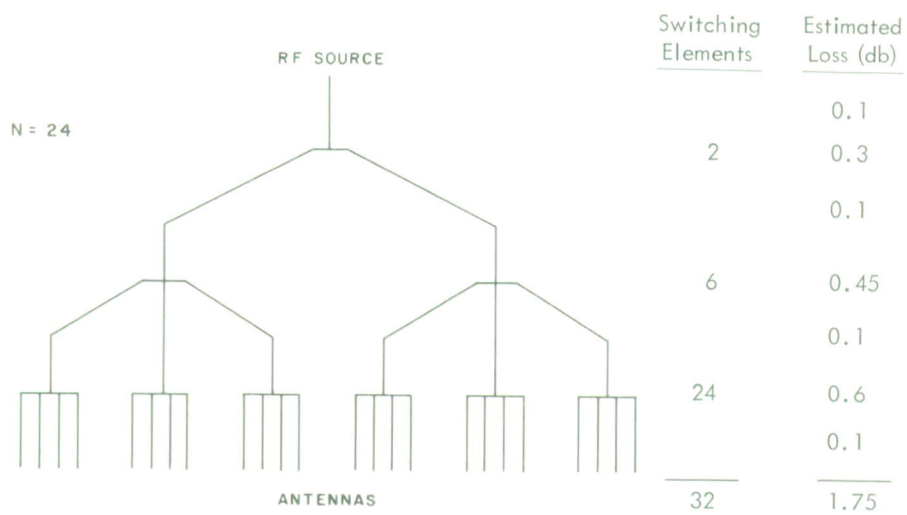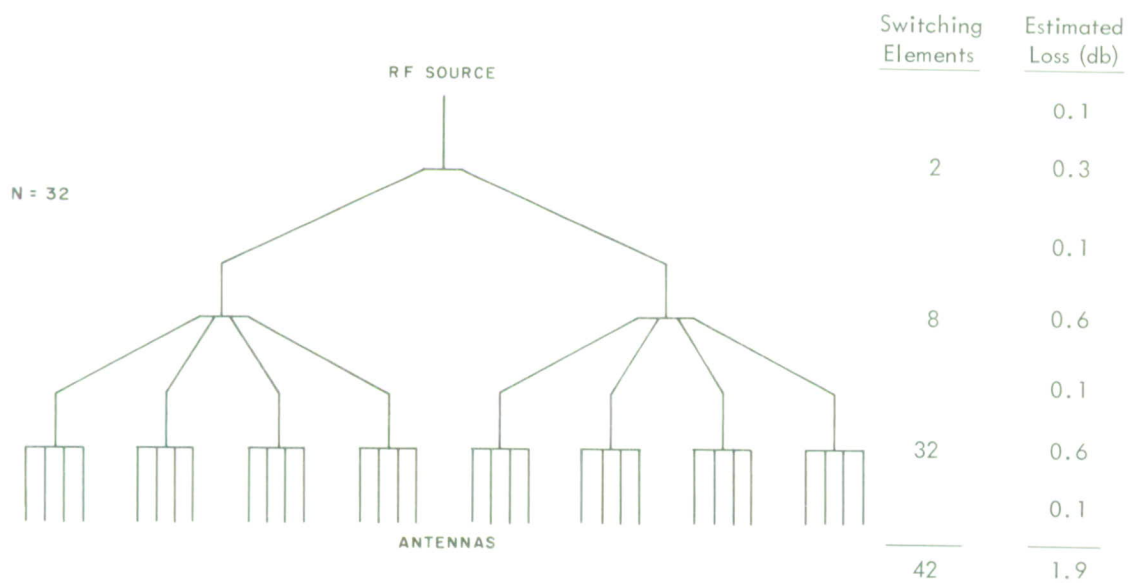
(g) 32-antenna system.

Fig. 27. Continued.
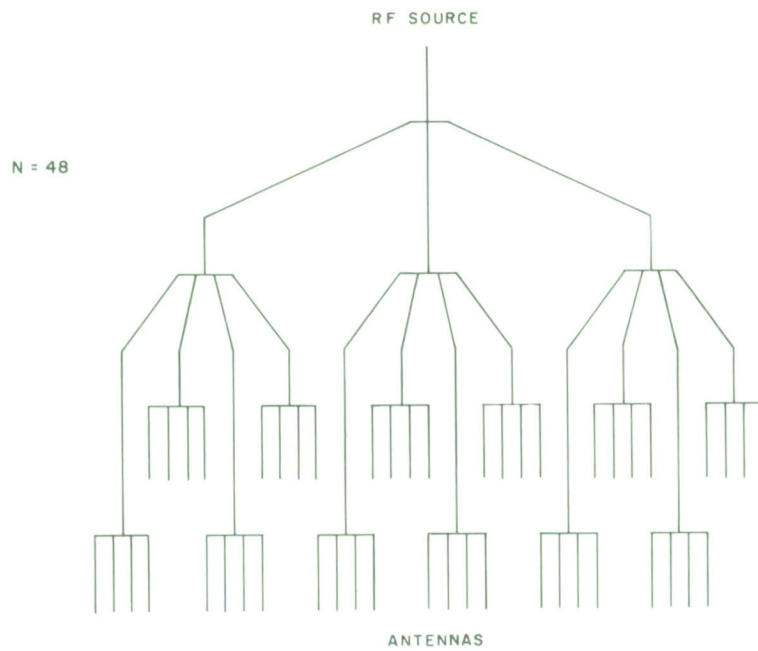
(h) 48-antenna system.

Switching Elements	Estimated Loss (db)
3	0.1
	0.45
	0.1
12	0.6
	0.1
48	0.6
	0.1
63	2.05

N = 48

RF SOURCE

ANTENNAS
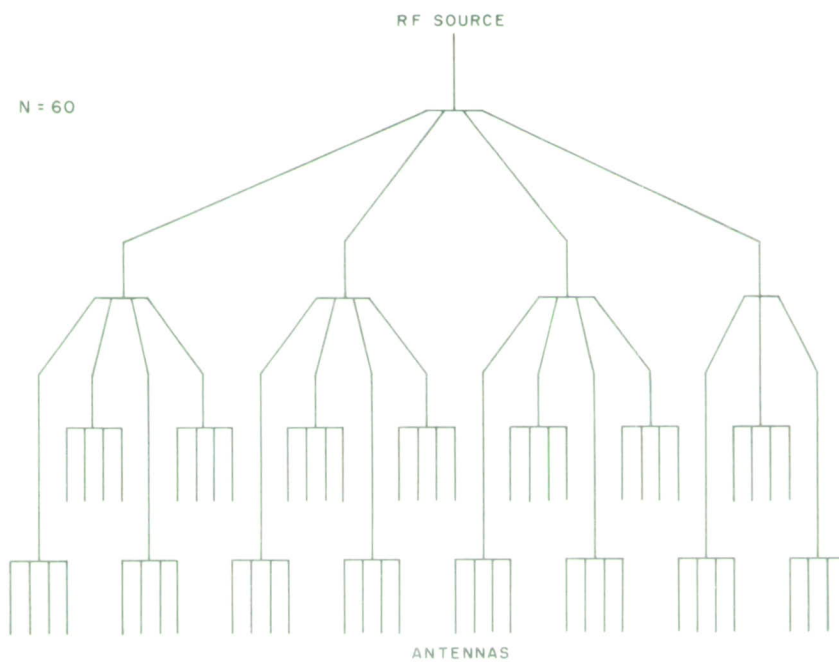
(i) 60-antenna system.

Switching Elements	Estimated Loss (db)
	0.1
4	0.6
	0.1
15	0.6
	0.1
60	0.6
	0.1
79	2.2

N = 60

RF SOURCE

ANTENNAS

Fig. 27. Continued.

ACKNOWLEDGMENTS

APPENDIX A

SUMMARY OF EXPECTED CHARACTERISTICS FOR CASES INVESTIGATED										
Number of Antennas N	4	6	8	12	16	24	32 Case 2	32 Case 1	48	60
Number of switching elements	4	8	10	15	20	32	42	42	63	79
Estimated circuit loss (db)	0.8	1.0	1.2	1.3	1.5	1.8	1.9	1.9	2.0	2.2
$\beta = 0°$ (angle between receiver and sensing direction)										
Largest possible angle of receiver from axis of operating antenna (deg)	70.5	54.7	49.9	37.4	33.8	27.7	22.7	23.9	19.1	16.9
This angle if angles between adjacent pointing directions could be made equal (ideal case) (deg)	70.5	54.7	46.5	37.4	32.1	26.1	22.5	22.5	18.3	16.3
Maximum antenna gain at this angle (db)	1.83	3.08	3.65	5.66	6.42	7.98	9.60	9.18	11.03	12.03
Gain at this angle after deducting circuit loss (db)	1.0	2.1	2.4	4.4	4.9	6.2	7.7	7.3	9.0	9.8
Antenna gain at peak for same antenna pattern (db)	5.81	7.06	7.63	9.64	10.40	11.96	13.58	13.16	15.01	16.01
Gain at peak after deducting circuit loss (db)	5.0	6.1	6.4	8.3	8.9	10.2	11.7	11.3	13.0	13.8
Half-power beamwidth for same pattern (deg)	111.7	91.6	84.4	64.4	58.4	48.2	39.6	41.6	33.4	29.6
$\beta = 8°$										
Largest possible angle of receiver from axis of operating antenna (deg)	78.5	62.7	57.9	45.4	41.8	35.7	30.7	31.9	27.1	24.9
Maximum antenna gain at this angle (db)	1.50	2.35	2.76	4.27	4.85	6.00	7.16	6.87	8.15	8.82
Gain at this angle after deducting circuit loss (db)	0.7	1.3	1.6	3.0	3.3	4.2	5.3	5.0	6.1	6.6
Antenna gain at peak for same antenna pattern (db)	5.48	6.33	6.74	8.25	8.83	9.98	11.14	10.85	12.13	12.80
Gain at peak after deducting circuit loss (db)	4.7	5.3	5.5	6.9	7.3	8.2	9.2	8.9	10.1	10.6
Half-power beamwidth for same pattern (deg)	118.7	102.6	96.1	77.3	71.6	61.6	53.2	55.2	47.1	43.5

DERIVATION OF THE FORMULA FOR ℓ_s/ℓ_c, WHERE $|a - \beta| < \gamma < a + \beta$

If $a - \beta < \gamma < a + \beta$ and $a > \beta$, or $\beta - a < \gamma < a + \beta$ and $a \leqslant \beta$, then there will be two directions OP_1 and OP_2 on the cone $ROS° = \beta$ where $POT° = a$ (Fig. B-1). Let points P_1, P_2, S, and T lie on a plane perpendicular to OS. The ratio ℓ_s/ℓ_c becomes simply the ratio of the angle subtended by the arc P_1P_2 at S to 2π, or

$$\frac{\ell_s}{\ell_c} = \frac{2P_1ST°}{2\pi} \qquad . \tag{B-1}$$

Now

$$P_1ST° = \cos^{-1} \frac{\overline{P_1S}^2 + \overline{ST}^2 - \overline{P_1T}^2}{2\overline{P_1S} \cdot \overline{ST}} \qquad . \tag{B-2}$$

Also

$$\overline{P_1T}^2 = \overline{OP_1}^2 + \overline{OT}^2 - 2\overline{OP_1} \cdot \overline{OT} \cos a \qquad . \tag{B-3}$$

Hence,

$$P_1ST° = \cos^{-1} \frac{\overline{P_1S}^2 + \overline{ST}^2 - \overline{OP_1}^2 - \overline{OT}^2 + 2\overline{OP_1} \cdot \overline{OT} \cos a}{2\overline{P_1S} \cdot \overline{ST}} \tag{B-4}$$

But

$$P_1S = OS \tan\beta \qquad , \tag{B-5}$$

$$ST = OS \tan\gamma \qquad , \tag{B-6}$$

$$OP_1 = OS \sec\beta \tag{B-7}$$

and

$$OT = OS \sec\gamma \qquad . \tag{B-8}$$

3-62-2621

Fig. B-1. Details of the geometry for the purpose of determining ℓ_s/ℓ_c when $|a - \beta| < \gamma < a + \beta$.

37
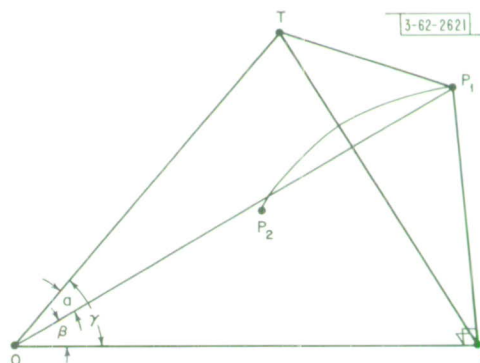
Hence,

$$P_1 ST° = \cos^{-1} \frac{\tan^2\beta + \tan^2\gamma - \sec^2\beta - \sec^2\gamma + 2\sec\beta\sec\gamma\cos a}{2\tan\beta\tan\gamma}$$

and this simplifies

$$P_1 ST° = \cos^{-1} \left(\frac{\cos a - \cos\beta\cos\gamma}{\sin\beta\sin\gamma}\right) \qquad . \tag{B-9}$$

Therefore,

$$\frac{\ell_s}{\ell_c} = \frac{1}{\pi}\cos^{-1}\frac{\cos a - \cos\beta\cos\gamma}{\sin\beta\sin\gamma} \qquad . \tag{B-10}$$

APPENDIX C
DERIVATION OF THE VALUE OF THE ANGLE v_{nij}

Referring to Fig. 4, one begins with the relation

$$\cos \Theta_{nib} = \frac{TF_i}{TG_{ij}} \quad . \tag{C-1}$$

But

$$TF_i = OT \tan u_{ni} \tag{C-2}$$

and

$$TG_{ij} = OT \tan v_{nij} \quad . \tag{C-3}$$

Hence,

$$\cos \Theta_{nib} = \frac{\tan u_{ni}}{\tan v_{nij}} \quad . \tag{C-4}$$

Similarly,

$$\cos \Theta_{nja} = \frac{\tan u_{nj}}{\tan v_{nij}} \quad . \tag{C-5}$$

Take the identity,

$$\sin \Theta_{nib} \sin \Theta_{nja} = \cos \Theta_{nib} \cos \Theta_{nja} - \cos (\Theta_{nib} + \Theta_{nja}) \quad , \tag{C-6}$$

square, substitute

$$\sin^2 \Theta_{nib} = 1 - \cos^2 \Theta_{nib} \tag{C-7}$$

and

$$\sin^2 \Theta_{nja} = 1 - \cos^2 \Theta_{nja} \quad , \tag{C-8}$$

and simplify. The result is

$$1 - \cos^2 \Theta_{nib} - \cos^2 \Theta_{nja} = - 2 \cos \Theta_{nib} \cos \Theta_{nja} \cos (\Theta_{nib} + \Theta_{nja})$$
$$+ \cos^2 (\Theta_{nib} + \Theta_{nja}) \quad . \tag{C-9}$$

When we substitute Eqs. (C-4) and (C-5) and solve for $\tan^2 v_{nij}$, the result is

$$\tan^2 v_{nij} = \frac{\tan^2 u_{ni} + \tan^2 u_{nj} - 2 \tan u_{ni} \tan u_{nj} \cos (\Theta_{nib} + \Theta_{nja})}{1 - \cos^2 (\Theta_{nib} + \Theta_{nja})} \quad . \tag{C-10}$$

But from Eqs. (20) and (21)

$$\cos (\Theta_{nib} + \Theta_{nja}) = \frac{\cos 2 u_{nij} - \cos 2 u_{ni} \cos 2 u_{nj}}{\sin 2 u_{ni} \sin 2 u_{nj}} \quad . \tag{C-11}$$

Also

$$\tan u_{ni} = \frac{1 - \cos 2 u_{ni}}{\sin 2 u_{ni}} \qquad (C-12)$$

and

$$\tan u_{nj} = \frac{1 - \cos 2 u_{nj}}{\sin 2 u_{nj}} \; . \qquad (C-13)$$

Equations (C-11) to (C-13) are substituted into Eq. (C-10), the numerator and denominator are multiplied by $\sin^2 2 u_{ni} \sin^2 2 u_{nj}$, and the result is

$$\tan^2 v_{nij} = (1 - \cos 2u_{ni})^2 \sin^2 2u_{nj} + (1 - \cos 2u_{nj})^2 \sin^2 2u_{ni}$$

$$\frac{-2 \, (1 - \cos 2u_{ni}) \, (1 - \cos 2u_{nj}) \, (\cos 2u_{nij} - \cos 2u_{ni} \cos 2u_{nj})}{\sin^2 2u_{ni} \sin^2 2u_{nj} - (\cos 2u_{nij} - \cos 2u_{ni} \cos 2u_{nj})^2} \; . \qquad (C-14)$$

By substituting

$$\sin^2 2u_{ni} = 1 - \cos^2 2u_{ni} \qquad (C-15)$$

and

$$\sin^2 2u_{nj} = 1 - \cos^2 2u_{nj} \; , \qquad (C-16)$$

Eq. (C-14) simplifies to

$$\tan^2 v_{nij} = \frac{2 \, (1 - \cos 2u_{ni}) \, (1 - \cos 2u_{nj}) \, (1 - \cos 2u_{nij})}{1 - \cos^2 2u_{ni} - \cos^2 2u_{nj} - \cos^2 2u_{nij} + 2 \cos 2u_{ni} \cos 2u_{nj} \cos 2u_{nij}} \; . \qquad (C-17)$$

APPENDIX D

COMPUTER PROGRAM TO CALCULATE PROBABILITY

Reading input data

Read in N, M, B_o, $D\beta$, $N\beta$, $D\alpha$, $D\gamma$

m = 1, M

Read in x(m), y(m), z(m), n(m), l(m), x_a(m,i), y_a(m,i), z_a(m,i), i = 1, l(m)

Calculation of constants of the geometry

V = 0

m = 1, M

U(m) = 1, i = l(m)

i = 1, 1

$$\cos 2u(m,i) = x(m)\, x_a(m,i) + y(m)\, y_a(m,i) + z(m)\, z_a(m,i)$$
$$\sin 2u(m,i) = \sqrt{1 - \cos^2 2u(m,i)}$$
$$\tan u(m,i) = \sin 2u(m,i)/[1 + \cos 2u(m,i)]$$
$$u(m,i) = \cos^{-1}[\cos 2u(m,i)]/2$$
$$e(m,i) = 2$$

Equation (8a)

Search for smallest u(m,i) for each m

u(m,i) − U(m)

U(m) = u(m,i)

i − 1

i = i − 1

i = 1

Setting of value of i

A

42

$$\cos_a 2U(m,i) = x_a(m,i)\, x_a(m,i) + y_a(m,i)\, y_a(m,i) + z_a(m,i)\, z_a(m,i)$$

$$v(m,i) = \tan^{-1} \sqrt{\frac{2|1 - \cos 2U(m,i)|\,|1 - \cos_a 2U(m,i)|}{1 - \cos^2 2U(m,i) - \cos_a^2 2U(m,i) + 2\cos 2U(m,i)\,\cos_a 2U(m,i)}}$$

$$\overline{\phi + \phi(m,i)} = \cos^{-1}\frac{\cos_a 2U(m,i) - \cos 2U(m,i)\,\cos 2U(m,i)}{\sin 2U(m,i)\,\sin 2U(m,i)}$$

Equations (8b), (21) and (22)

Search for largest v(m,i)

Lower limits of α and β

Lower limit of γ

V = v(m,i)

v(m,i) − V

β = β₀, α = 0

L = 1, Nβ

Write out β

cos β, sin β

p = 0, cos α

α − β

γ = 0

γ = β − α

S = 0, m, sin γ

Calculation loop for each value of β

Calculation loop for each value of α

Integration loop

A   B   C   D

Calculation of appropriate value of ℓ_s/ℓ_c

$$\frac{\ell_s}{\ell_c} = \frac{1}{\pi}\cos^{-1}\frac{\cos\alpha - \cos\beta\cos\gamma}{\sin\beta\sin\gamma}$$

$\cos\gamma$

$\gamma - (\alpha - \beta)$

$+$ 0 $-$

$\dfrac{\ell_s}{\ell_c} = 1$

$S_i = 0$
$\tan\gamma$
$l = l(m)$

$m = 1, M$

$\gamma - U(m)$

$+$ 0 $-$

Setting of value of i

$i = 1, I$

$i - I$

$+$ 0 $-$

$i = 1$

$i = i + 1$

Contribution to sum if $\gamma > v(m, i)$ and adjustment of value of $e(m, i)$

$\gamma - v(m, i)$

$+$ 0 $-$

$S_i = S_i + \phi^+ \phi(m, i)$
$e(m, i) = e(m, i) - 1$
$e(m, i) = e(m, i) - 1$

No contribution to sum if $e(m, i) = 0$ or $\gamma \leqslant u(m, i)$

$i = 1, I$

$e(m, i)$

$+$ 0 $-$

$\gamma - u(m, i)$

$+$ 0 $-$

Contribution to sum if $e(m, i) \neq 0$ and $\gamma > u(m, i)$

$S_i = S_i + e(m, i)\cos^{-1}[\tan u(m, i)/\tan\gamma]$

Summation over values of m

Omission of summations over i if $\gamma \leqslant U(m)$

Summation over values of i

Summation over values of i

E

F

G

D

C

B

44

3-62-2622(d)

$$S_m = S_m + n(m)\, S_i$$

$$P = P + \frac{f_s}{f_c}\left(\frac{N}{2} - \frac{S_m}{4\pi}\right)\sin\gamma$$

$$\gamma = \gamma + D\gamma$$

Contribution to integrand is added

Upper limit of γ

$\gamma - (\alpha + \beta)$

$\gamma - V$

$$P = P \times D\gamma$$

Final probability value

Write out α, P

$\alpha - (\beta + V)$

Upper limit of α

$\beta = \beta + D\beta$

$\alpha = \alpha + D\alpha$

End

A B C D E F

45